Nematology, 2010, Vol. 12(4), 519-542

Ultrastructure and life history of *Myolaimus byersi* n. sp. (Myolaimina: Myolaimidae), a phoretic associate of the crane fly, *Limonia schwarzi* (Alexander) (Limoniidae), in Florida

Robin M. GIBLIN-DAVIS [1,*], Natsumi KANZAKI [1,2], Paul DE LEY [3], Donna S. WILLIAMS [4], Einhard SCHIERENBERG [5], Erik J. RAGSDALE [3], Yongsan ZENG [1,6] and Barbara J. CENTER [1]

[1] *Fort Lauderdale Research and Education Center, University of Florida-IFAS, 3205 College Avenue, Fort Lauderdale, FL 33314-7719, USA*
[2] *Forest Pathology Laboratory, Forestry and Forest Product Research Institute, 1 Matsunosato, Tsukuba, Ibaraki, 305-8687, Japan*
[3] *Department of Nematology, University of California, Riverside, CA 92521, USA*
[4] *Department of Microbiology and Cell Science, University of Florida-IFAS, P.O. Box 110700, Gainesville, FL 32611-0700, USA*
[5] *Zoological Institute, University of Cologne, D-50923 Köln, Germany*
[6] *Nature and Environmental Department, Zhongkai University of Agriculture and Technology, Guangzhou, China*

Received: 26 June 2009; revised: 19 August 2009
Accepted for publication: 20 August 2009

Summary – *Myolaimus byersi* n. sp., a phoretic associate of the crane fly, *Limonia* (*Rhipidia*) *schwarzi* (Diptera: Limoniidae), was recovered from moist and decaying tissue from the crown shaft of a living spindle palm, *Hyophorbe verschaffeltii*, in southern Florida and is described herein. Dauers were carried in the abdominal folds of male and female *L. schwarzi*. Examination of the highly mobile crane fly larvae and pupae confirmed that the dauers were externally associated with the cuticle. Dauers from crane flies were culturable to adults on 1/20 strength TSB agar. The association appears to be relatively host specific. SEM studies, early embryonic development, dauers, molecular data and TEM ultrastructural comparisons of the stoma, sensory structures and sperm are used to discuss the relative placement of *Myolaimus* within the Nematoda. The stoma resembles diplogastrids in being strongly anisomorphic with an enlarged dorsal sector of the stegostom, yet also resembles rhabditids in having three triangular flaps in the metastegostom and matches cephalobs and panagrolaims in having a pharyngeal collar with two sets of three interradial muscles followed by two sets of six adradial muscles. The ultrastructure of the cheilostom epidermis shows a high degree of conservation with several Rhabditida. The sperm of *M. byersi* n. sp. is nearly identical to that of *Caenorhabditis elegans.* In early cell division, *M. byersi* n. sp. is closest to *Parascaris equorum* followed by *C. elegans*. *Myolaimus* apparently represents a divergent lineage that has followed a non-coalescing trajectory for a long time, allowing it to retain some highly conserved characters while also developing some surprisingly unique features, such as a baggy cuticle and males that lack a gubernaculum or spicules.

Keywords – bionomics, description, embryology, morphology, morphometrics, phoresy, phylogeny, systematics, taxonomy.

A living spindle palm, *Hyophorbe verschaffeltii* H. Wendl., in southern Florida was observed with an active localised infestation of the West Indian sugarcane weevil, *Metamasius hemipterus sericeus* (Olivier) (Coleoptera: Curculionidae) at 1.5 m above the soil line in the crown shaft. A subsample of this tissue was extracted and revealed a variety of free-living nematodes, including a species of *Myolaimus* Cobb, 1920 (referred to as *M. heterurus* in Giblin-Davis, 1997). *Myolaimus* is very interesting because it is the only known free-living nematode that has evolved a unique mating strategy involving the loss of its gubernaculum and spicules (Fürst von Lieven *et al.*, 2005), the copulatory structures used by almost all other male nematodes to anchor and mate with females. In addition, members of the genus possess a uniquely baggy cuticle that drapes loosely around

* Corresponding author, e-mail: giblin@ufl.edu

DOI:10.1163/138855409X12519673803912

living and moving animals. De Ley and Blaxter (2002) placed *Myolaimus* into its own monotypic suborder and this was supported by Nadler *et al*. (2006) with molecular sequence data from LSU that placed *Brevibucca* sp. as a putative sister taxon. Because the rotting palm tissue harbouring this *Myolaimus* sp. was sufficiently isolated from the soil (>1.3 m), it was hypothesised to have been introduced into the site by arthropods associated with the rot. Examination of a number of different arthropods revealed that the crane fly, *Limonia* (*Rhipidia*) *schwarzi* (Alexander), was the sole phoretic host of this species of *Myolaimus* (Giblin-Davis, 1997). A xenic culture (RGD233) was established and the nematode was determined to be new to science and is described herein as *Myolaimus byersi* Giblin-Davis, Kanzaki & De Ley n. sp. Observations are also provided on its ultrastructure, development and relationships.

There are over 95 species of North American *Limonia* known from lentic (= standing water) or lotic (= running water) margins where they have been observed as semi-aquatic burrowers and sprawlers. Their larvae are widespread and function as herbivore shredders, often feeding by chewing on microalgae (Pritchard, 1983). *Limonia* (*R.*) *schwarzi* has a neotropical distribution and can be found in rotting plant tissue such as decomposing banana, sugarcane and palm. Eggs are laid in a suitable medium and eclose within a week before completing four larval instars to the mobile pupal stage, which lasts for about 5-6 days (Byers, pers. comm.). This species is multivoltine with several overlapping generations per year. There have been relatively few reports of nematodes associated with the more than 14 000 species of Tipuloidea worldwide and most of these have been thelastomatids, which are gut parasites (see Poinar, 1975). Byers (1983) reported an apparently phoretic association between the snow fly, *Chionea alexandriana* Garrett, from an abandoned nest of the pack rat, *Neotoma cinerea* (Ord), in Northern California and an undescribed species of *Rhabditis* which, as a gravid female, apparently lays an egg mass or wraps itself around the neck of a dispersing fly to gain transportation to the next rat nest. Until recently, *Myolaimus* was not known to be associated with insects at all (Giblin-Davis, 1997) and was reported mostly in association with moist or aquatic environments and rotting timber or vegetation, including compost piles (Hirschmann, 1952; Paesler, 1956; Andrássy, 1959). We report here in detail on the association between *M. byersi* n. sp. and its carrier *L.* (*R.*) *schwarzi*, with description of the phoretic dauer stage and first observations on embryogenesis and ultrastructural features of this remarkable nematode.

Materials and methods

Sampling and culturing of the nematode

Rotting tissue was harvested from the crown shaft of a still living spindle palm, *H. verschaffeltii*, at the University of Florida, Fort Lauderdale Research and Education Center, Davie, Florida, and subjected to nematode extraction using a Baermann funnel (Southey, 1970). Several individuals of *M. byersi* n. sp. were hand-picked onto 1/20 strength tryptic soy broth agar (TSB) to establish a xenic culture (RGD233) on 9 March, 1996. Since then, this culture has been maintained in the laboratory with bi-weekly subculturing onto 1/20 strength tryptic soy broth agar (TSB) at room temperature (*ca* 24°C).

Molecular profiles

Nematodes were handpicked live into distilled water and some of them were stored in modified Worm Lysis Buffer (WLB: Williams *et al.*, 1992; Ye *et al.*, 2007) for DNA extraction, amplification and sequencing attempts, or collected, heat-killed and placed into 5% formalin for measurements by light microscopy and then processed into 100% glycerin for permanent vouchers (Southey, 1970).

Nematode samples that had been stored in WLB were digested and stored at −20°C until used as a PCR template for the small subunit (SSU) rRNA gene which was amplified and sequenced as described by Ye *et al.* (2007). In addition, a culture of *M. byersi* n. sp. (RGD233) was made available to Nadler *et al.* (2006), who sequenced two non-contiguous fragments of the LSU of this isolate, which are available as DQ145643 and DQ145691 in the GenBank database.

Morphological observation and measurement

Adults of *M. byersi* n. sp. were collected from 11- to 14-day-old cultures and heat-killed for measurements in temporary water mounts. Other specimens were fixed in formalin-glycerin for longer than 24 h and processed slowly to glycerin before making permanent slides and measurements (Southey, 1970). Nematodes were drawn and measured with the aid of a camera lucida and a stage micrometer. Photomicrographs were taken with an Olympus E-410 attached to the phototube of an Olympus

BH-2 microscope and edited using Adobe Photoshop Elements 2.0.

Scanning electron microscopy (SEM)

The external morphology of adults of both sexes of *M. byersi* n. sp. and an adult female of *L. schwarzi* was examined with SEM. Specimens were fixed in 3% (v/v) glutaraldehyde, post-fixed in 2% OsO_4 for 12 h at 22°C, rinsed in dH_2O, dehydrated in a graded ethanol series, critical point dried from liquid CO_2, mounted on a stub with double sticky tape, sputter-coated with 20 nm of gold-palladium and viewed with a Hitachi S-4000 Field Emission SEM at 7 kV.

Transmission electron microscopy (TEM)

Nematode specimens were collected live into 2% formaldehyde (prepared from paraformaldehyde) and 2.5% glutaraldehyde in 0.1 M cacodylate buffer at pH 7.2 and fixed overnight at 4°C. After repeated rinsing in buffer, specimens were postfixed in 2% OsO_4 in 0.1 M cacodylate buffer at pH 7.2 for 3.5 h at 22°C. Nematodes were rinsed in water, fixed with 1% aqueous uranyl acetate, dehydrated through 100% ethanol into 100% acetone and infiltrated with Spurr's epoxy resin. Blocks were sectioned on a RMC® MT-6000-XL ultra-microtome and nearly serial sections with silver refraction (75 nm) were picked up on copper grids having a 0.35% Formvar coating reinforced with a light carbon film. Sections were post-stained with 5% aqueous uranyl acetate and lead citrate before viewing on a Zeiss EM-10CA® transmission electron microscope at 80 kV. One adult male and female nematode were each transverse-sectioned and another male and female nematode were each sagittally-sectioned through the stoma and anterior pharynx. In addition, a mating couple was sectioned for examination of sperm and other features, such as the baggy cuticle.

Embryonic development

Eggs in the single cell stage were removed from females of *M. byersi* n. sp., placed onto a microscopic slide on a thin layer of water agar, covered with a cover slip and sealed with petroleum jelly. Embryonic development was monitored with a Leitz Orthoplan microscope with differential interference optics (DIC) using a 100× Plan objective and recorded with a high-resolution video camera to help reconstruct the early embryonic development. (Schierenberg, 1984).

Insect association

An additional 300 ml of rotting palm tissue was collected from the original spindle palm that was found to harbour *M. byersi* n. sp. The tissue was placed in each of three high-density polyethylene (HDPE) 0.9-l plastic, tapered containers with screened lids to retain emerging insects (8.5 cm screened opening). These cages were observed almost daily for 45 days and water was added to prevent desiccation. Any invertebrates found on the surface or flying to the screen were dissected and examined for nematode associates. Any dauers that were observed were recorded for their location on or inside the invertebrate carrier and transferred to TSB media for culture comparisons with adults from the RGD233 culture for identity confirmation. A subsampling of dauers was used for morphological examination and morphometrics. In addition, some of the infested palm tissue was harvested to examine immatures of the suspected carrier of the nematode and to observe details of the nature of the association.

Paraffin sectioning

Several newly emerged adult *L. schwarzi* from the *M. byersi* n. sp. infested rotting palm tissue were heat-killed and fixed in FAA (formalin/acetic acid/ethanol = 5 : 5 : 90) for several days and then dehydrated in a tertiary butyl alcohol series and embedded in paraffin as per the method of Johansen (1940). Embedded flies were sectioned 11 μm thick, mounted on slides treated with Mayer's albumin (50 ml fresh egg albumin, 50 ml glycerin, 1 g sodium salicylate), stained with 1% aqueous safranin for 90 min and 0.5% fast green in clove oil and 100% ethanol (1 : 1) for 15 s, before being examined and photographed with a compound photomicroscope to confirm the location of association (Fig. 1).

Myolaimus byersi* **Giblin-Davis, Kanzaki & De Ley n. sp.**

= *M. heterurus apud* Giblin-Davis, 1997 *nec* Cobb, 1920

(Figs 2-6)

Measurements

See Table 1.

* The species is named in honour of Dr George W. Byers for a lifetime of contributions to the taxonomy and biology of the Tipuloidea and for his identification of the carrier of this nematode.

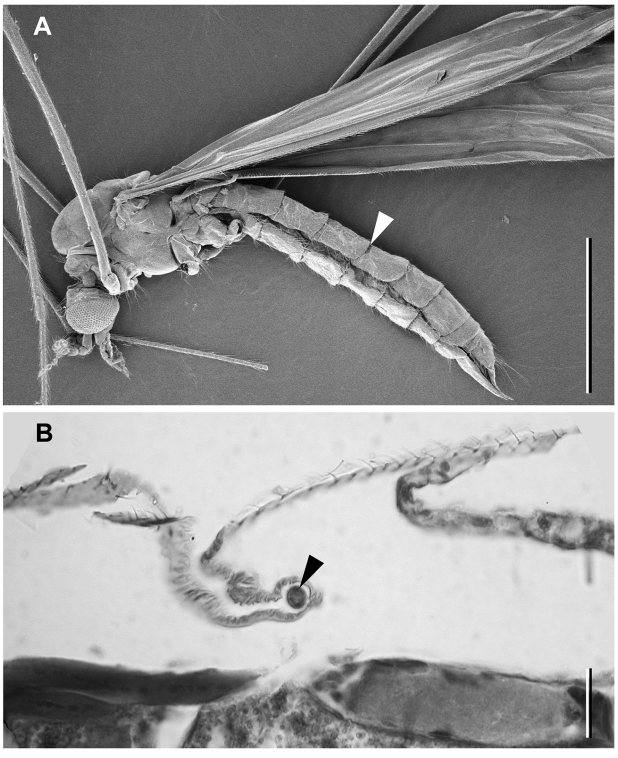

Fig. 1. *Adult female of* Limonia schwarzi*, the transport host of* Myolaimus byersi *n. sp. A: SEM of adult crane fly with one abdominal intersegmental transport region highlighted with white arrow (scale bar = 1.5 mm); B: Histological section through abdominal intersegmental fold with dauer of* M. byersi *n. sp. highlighted with black arrow (scale bar = 30 μm).*

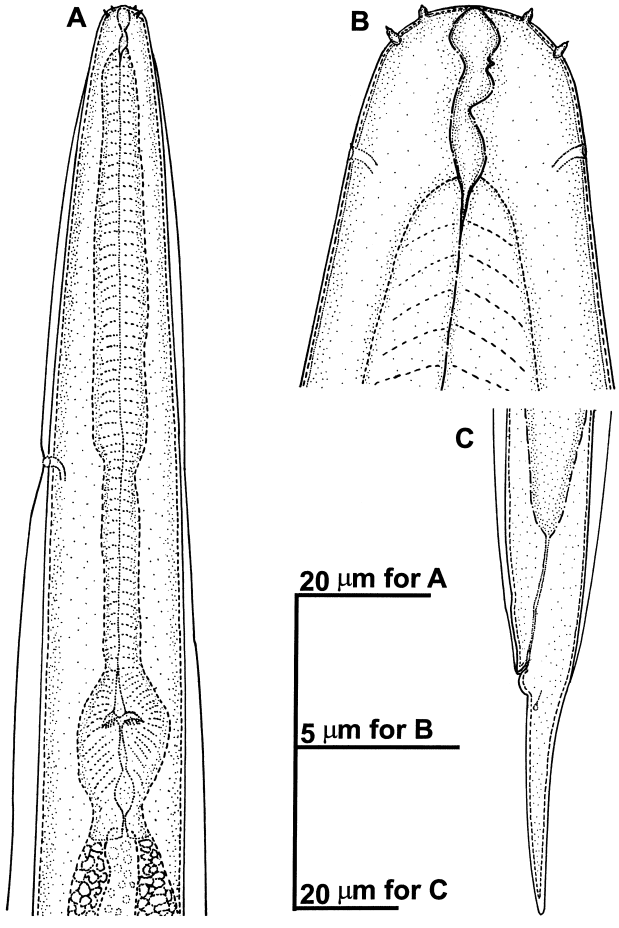

Fig. 2. *Dauer of* Myolaimus byersi *n. sp. A: Anterior region; B: Close-up of head; C: Tail region.*

DESCRIPTION

Male

Body medium length with slight, ventral arc when heat-killed. Tail region ventrally curved. Cuticle annulated, often appearing swollen and baggy with detached median layer. Lateral field not observed. Triradiate oral opening, indentation present at apex of each of three lip sectors, each sector bearing two setiform setae (*i.e.*, six in all). Four cephalic setae (longer than labial setae) present outside ring of labial setae, two at dorsal corners of dorsal sector and one medially on each subventral sector. Amphidial apertures elliptical, *ca* one head diam. posterior to head. Stoma *ca* twice as deep as broad, mostly composed of an anisomorphic, non-segmented, cheilostom. In lateral view, dorsal wall of cheilostom *ca* two-thirds length of ventral wall. Anisomorphic gymnostom joining cheilostom dorsally to produce an internally protuberant, tooth-like, ridge. Dorsal wall of gymnostom more than twice length of ventral wall in lateral view. Thus, cheilostom anisomorphy is counterbalanced by a reciprocal anisomorphy of the gymnostom giving the stoma general appearance of an isomorphic barrel in ventral or dorsal views. In lateral view, pharyngeal collar extending dorsally more anteriad than on subventral side. Prostegostom anisomorphic, being slightly longer dorsally than subventrally. Meso-, meta- and telostegostomatal elements appearing tube-like in lateral view with light microscopy. Anterior pharynx (procorpus + median bulb) long, muscular, nearly cylindrical. Pharynx panagrolaimoid. Posterior pharynx (isthmus + terminal bulb), shorter (*ca* 40% of total length of pharynx) than anterior pharynx, isthmus cylindrical, leading into distinctive basal bulb with grinder. Cardia small, not well developed. Hemizonid not observed. Nerve ring surrounding middle part of isthmus. Excretory pore opening near base to *ca* one corpus diam.

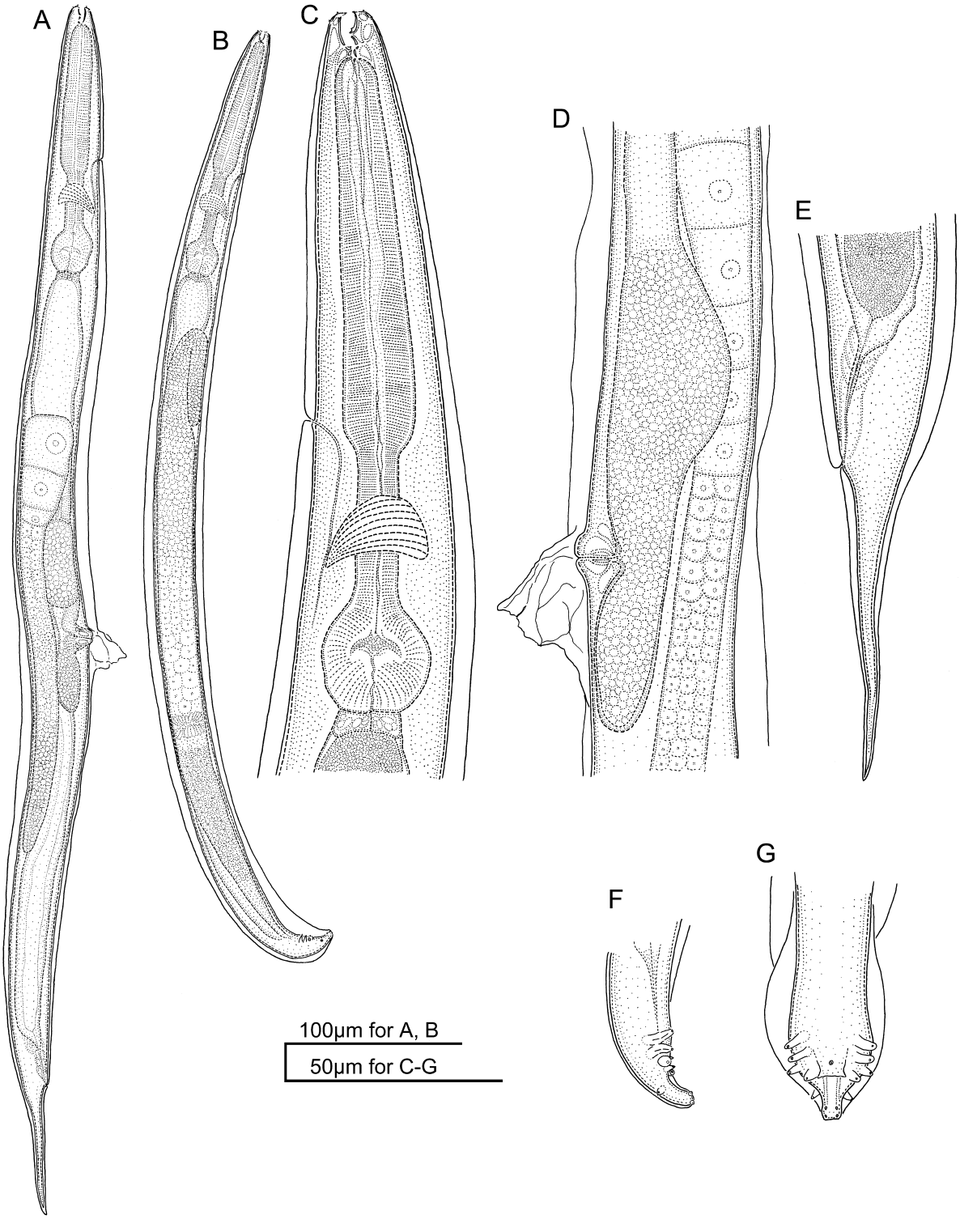

Fig. 3. *Lateral view of adults of* Myolaimus byersi *n. sp. A: Female; B: Male; C: Anterior region of female; D: Vaginal region; E: Tail region; F: Male tail region; G: Male tail region (ventral view).*

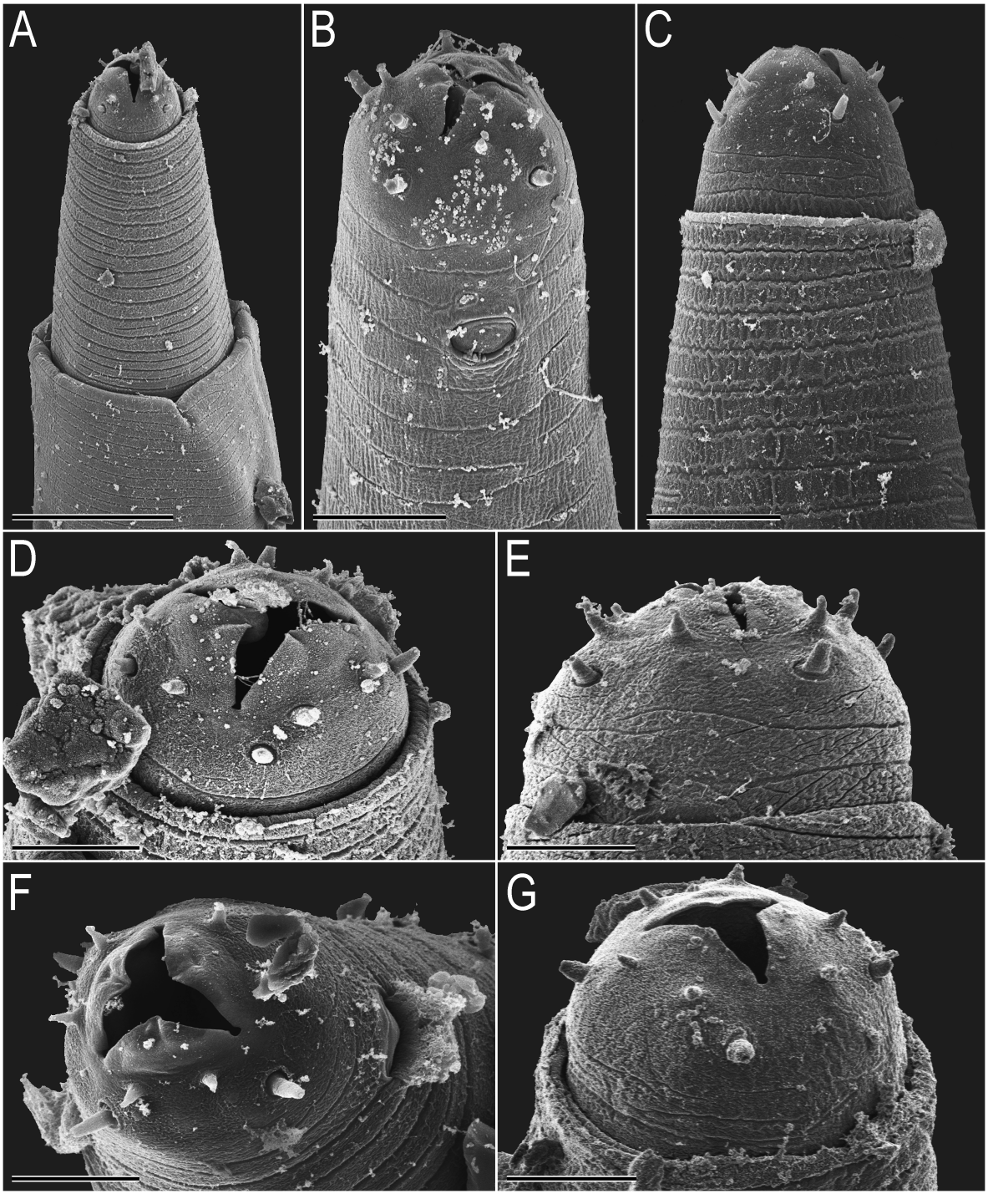

Fig. 4. *Scanning electron micrographs of head region of* Myolaimus byersi *n. sp. A: Female showing cuticular folds; B: Dorsolateral view of juvenile showing amphid; C: Lateral view of juvenile; D: Close-up of female head; E: Close-up of female head; F: Close-up of male head with amphids visible (with exudate); G: Close-up of male head with fold. (Scale: A = 9.7 μm; B = 2.2 μm; C = 2.9 μm; D = 1.9 μm; E, G = 1.8 μm; F = 1.5 μm.)*

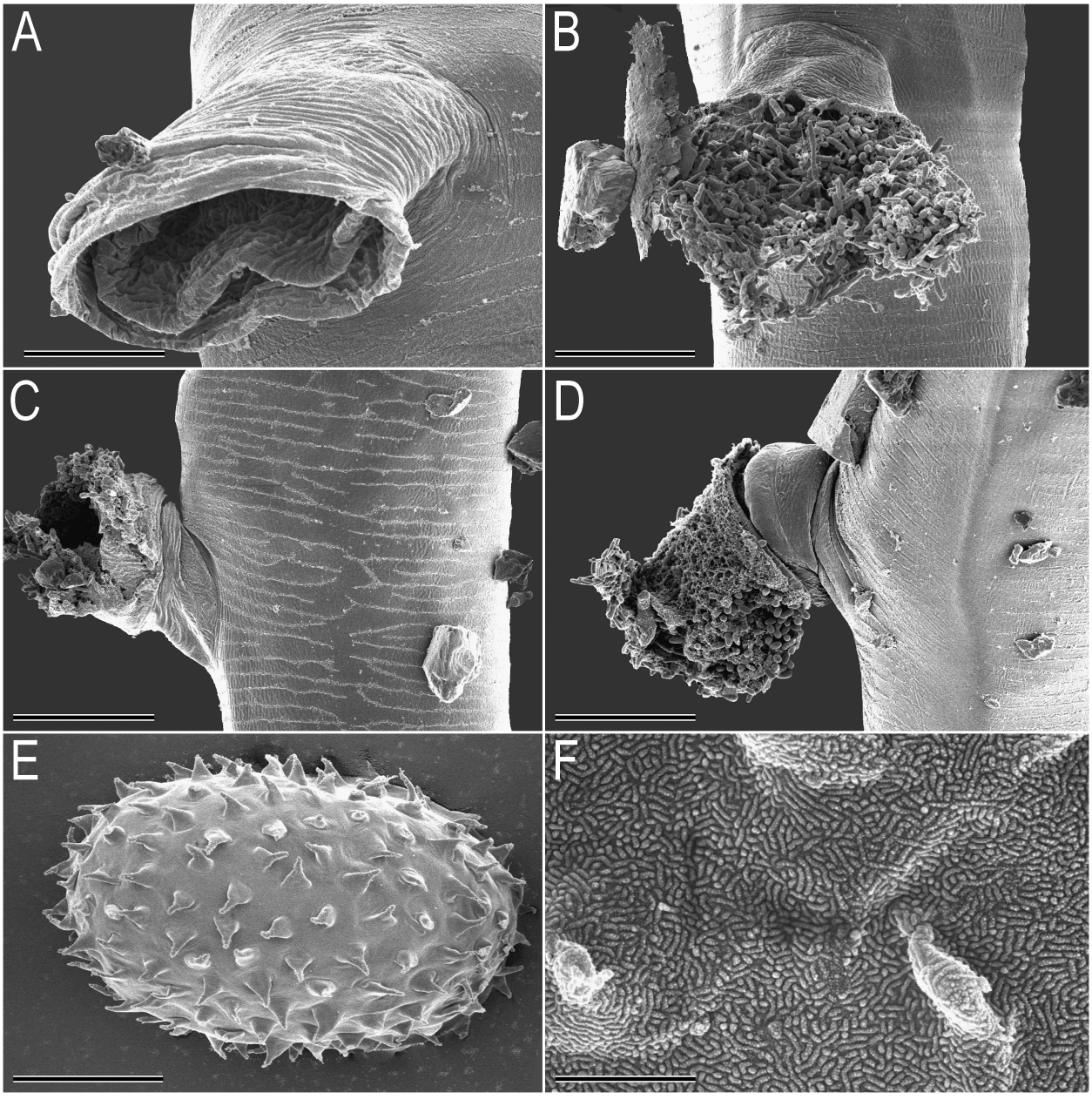

Fig. 5. *Scanning electron micrographs of female vulval region and egg of* Myolaimus byersi *n. sp. A: Vulva without spermatophore (sublateral view); B: Lateral view of vulva with spermatophore; C: Lateral view of female vulval region with spermatophore; D: Lateral view of vulval region with spermatophore of different female; E: Egg; F: Close-up of egg surface. (Scale: A = 3.3 μm; B = 6.7 μm; C, D = 7.8 μm; E = 7.3 μm; F = 0.7 μm.)*

anterior to base of corpus. Baggy cuticle always fully attached at excretory pore. Deirids usually distinct as a pair of mildly refringent and short conical projections located laterally at level of excretory pore. Testis reflexed for *ca* 15% of its length, spermatogonia, spermatocytes and spermatids arranged in multiple rows in anterior part, *vas deferens* not clearly distinguished, rod-like crystals encircling anterior region of *vas deferens* lumen. Spicules and gubernaculum absent. Tail hand-like in ventral view (analogous to strongylid bursa with rays), tip bluntly

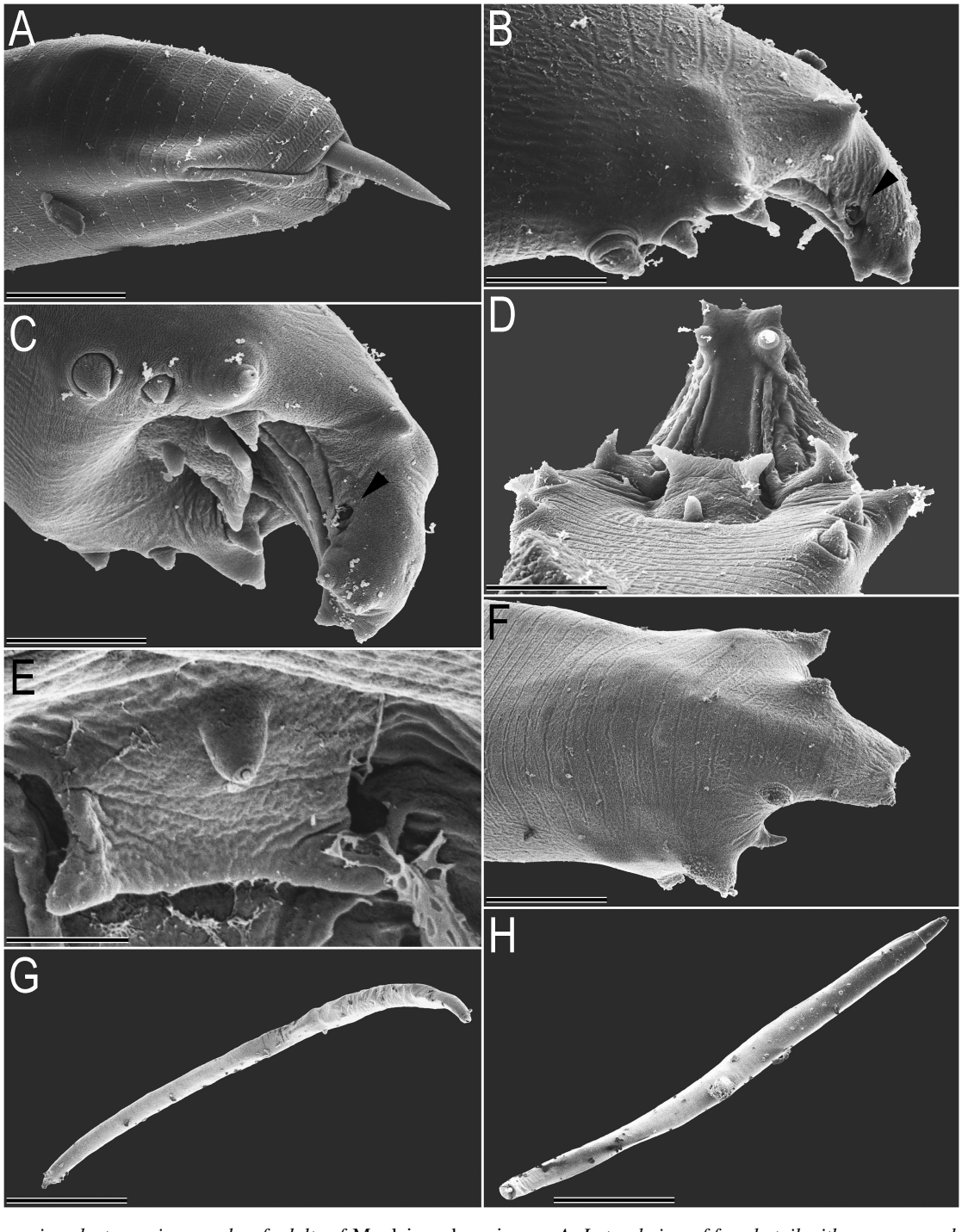

Fig. 6. *Scanning electron micrographs of adults of* Myolaimus byersi *n. sp. A: Lateral view of female tail with anus covered by baggy cuticle; B: Lateral view of male tail (arrowhead = phasmid); C: Ventro-lateral view of male tail (arrowhead = phasmid); D: Anterio-ventral view of male tail; E: Ventral view of pre-cloacal flap and papilla; F: Dorsal view of male tail; G: Subventral view of entire male; H: Ventral view of entire female. (Scale: A = 4.0 μm; B = 2.0 μm; C = 2.7 μm; D = 2.3 μm; E = 0.9 μm; F = 3.9 μm; G = 58 μm; H = 67 μm.)*

Table 1. *Morphometrics of* Myolaimus byersi *n. sp. All measurements are in μm and in the form: mean ± s.d. (range).*

Character	Holotype (glycerin)	Temporary water mount		
	Male	Male	Female	Dauer
n	–	16	16	10
L	510	537 ± 42 (474-606)	682 ± 62 (586-771)	518 ± 29 (475-556)
a	28.3	26.2 ± 1.4 (23.6-29.1)	23.8 ± 1.7 (21.9-27.4)	24.3 ± 3.6 (20.0-31.2)
b	3.8	3.7 ± 0.2 (3.3-4.0)	4.5 ± 0.5 (4.1-5.8)	4.1 ± 0.2 (3.7-4.6)
c	68.0	67.5 ± 7.5 (54.1-81.0)	12.3 ± 1.4 (9.9-14.8)	11.3 ± 1.2 (9.4-13.0)
c′	1.1	1.2 ± 0.1 (1.0-1.4)	5.2 ± 0.7 (3.8-6.5)	5.4 ± 1.1 (4.1-7.2)
V or T	69	72.4 ± 4.5 (65-81)	52.5 ± 1.7 (48.8-55.2)	–
Labial diam.	8.0	7.5 ± 0.5 (7.0-8.5)	8.5 ± 0.7 (7.5-10.0)	–
Stoma length	9.0	9.0 ± 1.3 (7.0-11.5)	12.0 ± 1.3 (9.0-13.0)	4.0, 2.0, 3.0, 4.0*
Anterior part of pharynx	83	74 ± 5.8 (63-85)	81 ± 8.8 (65-90)	65, 66, 60, 61*
Posterior part of pharynx	51	59 ± 3.7 (53-65)	57 ± 6.4 (38-66)	44, 39, 49, 49*
Excretory pore from anterior and	68	78 ± 4.7 (70-85)	84 ± 9.0 (63-99)	66 ± 3.7 (59-71)
Max. body diam.	18	21 ± 1.3 (18-24)	29 ± 3.1 (23-34)	22 ± 2.7 (18-25)
Vulval body diam. with tube	–	–	46 ± 1.6 (37-56)	–
Ovary or testis length	350	406 ± 55 (332-518)	260 ± 48 (186-332)	–
Post-uterine sac length	–	–	34 ± 2.0 (30-37)	–
Anal body diam.	6.8	6.5 ± 0.8 (5.5-8.0)	11.0 ± 1.4 (8.0-13.0)	9.0 ± 1.5 (6.0-10.0)
Tail length	7.5	8.0 ± 0.9 (7.0-10.0)	57 ± 9.4 (41-71)	46 ± 4.6 (41-52)

*: n = 4, because of the sample condition.

squared in lateral view, ventrally arcuate, dorsal cloacal wall heavily sclerotised; extending outwards to level of phasmids (posterior to GP5), appearing as shoehorn-like structure ending in a digitate tail tip with two pairs of terminal papillae (GP6-7). Cloacal aperture covered by large trapezoidal cloacal flap with bifurcate distal edge and single peg-like ventral papilla at its base. Complement of seven pairs of genital papillae present, first two pairs (GP1-2) large, equidistant from one another (both in sockets), GP3 located anterior to cloacal aperture, third and fourth pairs also large and digitate, almost at level of cloacal aperture in lateral view, GP3 being dorsolateral (without socket) and GP4 being ventral, GP5 located dorsally just anterior to phasmids, GP6-7 terminal on bluntly squared tail tip. Bursa absent, but cuticle often baggy around posterior end and can be mistaken for a bursa.

Female

Body usually straight when heat-killed. Cuticle and anterior region same as male, except that deirids usually not discernible, although in some specimens visible at level of excretory pore, apparently consisting only of a nerve ending, terminating just below basal layer of cuticle with no externally visible projection, swelling or pore. Ovary monodelphic, antidromously reflexed (= ovary reflexed for its entire length), extending *ca* 3.5 vulval body diam. posterior to vulva. Oocytes arranged in multiple rows in distal half but in single file in posterior part. Oviduct and uterus not clearly differentiated from one another, usually containing one egg. Egg with spiny coat. Post-uterine sac (PUS) present, *ca* one vulval body diam. long, sometimes containing sperm, cells of PUS with refractive granules in cytoplasm. Vulva slightly protuberant, with large, open, tube-like cuticular extension (vulval sac), *ca* one vulval body diam. long, often with copulation plug. Vagina located at mid-body, perpendicular to body surface. Rectum *ca* two anal body diam. long. Intestine-rectum junction constricted by sphincter muscle. Tail uniformly conoid, pointed at tip. Phasmids inconspicuous, pore-like, located *ca* one anal body diam. posterior to anus. Anus and most of tail often enveloped by baggy cuticle.

Dauer

Panagrolaimid-like. Body straight, tapering at both ends when heat-killed. Cuticle often appearing swollen and baggy with duplicature, especially around mid-body to tail region. Lateral field not observed. Amphidial aper-

tures small, elliptical, *ca* one head diam. posterior to mouth. Stoma closed, vestigial. Pharynx reduced in development, panagrolaimid-like; corpus long, nearly cylindrical, median bulb indistinct. Posterior pharynx (isthmus + terminal bulb), about same length as corpus, isthmus cylindrical, leading into distinctive basal bulb with reduced grinder. Cardia small, not well developed. Hemizonid not observed. Nerve ring indistinct, surrounding anterior to middle part of isthmus. Excretory pore opening near base of corpus. Rectum *ca* two anal body diam. long. Intestine-rectum junction constricted by sphincter muscle. Tail uniformly conoid, pointed at tip. Phasmid indistinct, pore-like, located *ca* one anal body diam. posterior to anus.

Type host and locality

Myolaimus byersi n. sp. (culture code RGD233) was isolated from rotting tissue of spindle palm (*Hyophorbe verschaffeltii*) coinfested by the crane fly *Limonia* (*Rhipidia*) *schwarzi* and collected at the Fort Lauderdale Research and Education Center, University of Florida, Davie, FL, USA, on 9 March, 1996.

Type material

Holotype male and four paratype males and four females deposited at the USDA Nematode Collection, Beltsville, MD, USA. Several paratype slides (same data as holotype) deposited at the University of California, Riverside, CA, USA, Fort Lauderdale Research and Education Center, University of Florida, Fort Lauderdale, FL, USA, and The Food and Environment Agency (FERA), York, UK.

Type cultures

Depositions of type cultures of RGD233 have been made with the *Caenorhabditis* Genetics Center (CGC; http://www.cbs.umn.edu/CGC/).

Diagnosis and relationships

Besides the generic apomorphies of a baggy cuticle, male lacking gubernaculum and spicules and female with long tube-like, cuticular vulval sac and eggs with spines, *M. byersi* n. sp. is characterised by a body length less than 800 μm, stoma longer than broad with pronounced anisomorphy, sexual dimorphism in the morphology of the deirids (short conical projections in males but difficult to observe in females), post-uterine sac one vulval body diam. long and possessing refractive granules within the cytoplasm of its cells, female tail uniformly conoid, sclerotisation of the dorsal cloacal wall extending to level of large pore-like phasmids (posterior to GP5) and manifested as a shoehorn-like structure ending in a digitate tail tip with two pairs of terminal papillae (GP6-7), cloacal aperture covered by large trapezoidal flap with bifurcate edge and single peg-like ventral papilla at its base and phoretic association with the crane fly, *L. schwarzi.*

The quantitative characters of the genus are highly variable within each of the nine nominal species; thus, *M. byersi* n. sp. is diagnosed mostly by qualitative typological characters. Overall, *M. byersi* n. sp. is based upon stomatal morphology most similar to *M. dendrodipnis* Paesler, 1956, *M. amititiae* Andrássy, 1959 and *M. rahmi* Sudhaus, 1977 (= *Cephalobus bursifer* Rahm, 1928). However it differs from *M. dendrodipnis* in the following features: female tail 3.8-6.5 anal body diam. long and uniformly conoid with pointed tip (Andrássy, 1984) *vs* 2-3 anal body diam. long with dorsal flexure and needle sharp tip; and cloaca covered by trapezoidal flap with single peg-like papilla at base and bifurcate distal edge *vs* no cloacal flap and no single peg-like papilla above level of cloaca. *Myolaimus byersi* n. sp. differs from *M. amititiae* in the non-segmented and anisomorphic cheilostom with the dorsal wall *ca* two-thirds as long as ventral wall *vs* cheilostom segmented and isomorphic; dorsal ridge in stoma formed by incurvature of cheilostom and gymnostom *vs* a dorsal ridge formed from the incurving gymnostom and mesostegostom with a metastegostom flap-like tooth; pharyngeal collar asymmetrical *vs* symmetrical; female tail tip pointed *vs* needle sharp; GP5 dorsal *vs* GP4 dorsal; and cloaca covered by trapezoidal flap with single peg-like papilla at base and bifurcate distal edge *vs* no cloacal flap and single peg-like papilla anterior to level of cloacal aperture and two small ventral peg-like papillae immediately following the cloacal aperture (although the two small ventral peg-like papillae might have been a misinterpretation of a bifurcate distal edge on a cloacal flap). *Myolaimus byersi* n. sp. is also close to *M. rahmi* which had the male illustrated in Figure 48 as a female (Rahm, 1928), but differs in body size of $<$800 *vs* $>$1200 μm; stoma twice *vs* thrice as long as broad; vagina located at mid-body *vs* at two-thirds of body length; male genital papillae arrangement 5 + ph + 2 *vs* 4+?. *Myolaimus byersi* n. sp. is also close to *M. maupasi* (= *Macrolaimus maupasi* Hnatewytsch, 1929) (Sanwal, 1960) but can be

distinguished from it by the following characters: amphids elliptical and *ca* one head diam. posterior to head *vs* circular and less than one head length posterior; dorsal ridge in stoma anterior to pharyngeal collar *vs* enveloped by pharyngeal collar; nerve ring surrounding middle part of isthmus *vs* at base of corpus; post-uterine sac *ca* one vulval body diam. long *vs* less than one vulval body diam. long; female tail uniformly conoid and straight *vs* finely tipped and dorsally reflexed; male genital papillae arrangement 5 + ph + 2 *vs* 4+?; and cloaca covered by trapezoidal flap with single peg-like papilla at base and bifurcate distal edge *vs* cloacal flap and papilla absent.

Myolaimus byersi n. sp. differs from *M. indicus* Ali, Farooqui & Suryawanshi, 1970 in post-uterine sac *ca* one vulval body diam. long *vs* less than one vulval body diam. long; female tail uniformly conoid, straight and shorter ($c' < 6.5$) *vs* finely tipped, dorsally reflexed and longer ($c' = 7$-8); males present *vs* not observed.

Myolaimus byersi n. sp. differs from *M. tepidus* Andrássy, 2005 in female tail uniformly conoid, straight and longer ($c' > 3.8$) *vs* uniformly conoid and short ($c' = 2.0$-2.5); genital papillae arrangement 5 + ph + 2 *vs* 4 ? + ph ? + 2 and cloaca covered by trapezoidal flap with single peg-like papilla at base and bifurcate distal edge *vs* cloacal flap and papilla absent.

Myolaimus byersi n. sp. differs from *M. heterurus* Cobb, 1920 (= *M. stiloides*) by the following characters: cheilostom anisomorphic with the dorsal wall *ca* two-thirds as long as ventral wall *vs* cheilostom isomorphic with some variability between the drawings of Cobb (1920), Weingärtner (1952) and Meyl (1954); post-uterine sac *ca* one vulval body diam. long *vs* longer than one vulval body diam. long; female tail uniformly conoid and straight *vs* finely tipped and variable; and cloacal aperture covered by trapezoidal flap with single peg-like papilla at base and bifurcate distal edge *vs* cloacal flap or papilla absent. *Myolaimus byersi* n. sp. can be separated from *M. goodeyorum* Andrássy, 1984 (= *M. heterurus*, according to Goodey, 1929) in that the cheilostom is anisomorphic with the dorsal wall *ca* two-thirds as long as ventral wall *vs* cheilostom isomorphic; dorsal ridge in stoma located anterior to pharyngeal collar *vs* enveloped by pharyngeal collar; post-uterine sac *ca* one vulval body diam. long *vs* longer than vulval body diam. long; female tail uniformly conoid and straight *vs* finely tipped and dorsally reflexed; cloaca covered by trapezoidal flap with single peg-like papilla at base and bifurcate distal edge *vs* cloacal flap and papilla absent.

Lastly, *M. byersi* n. sp. can be distinguished from *M. stammeri* Hirschmann, 1952 by the body (<800 *vs* >1000 μm long); stoma longer than broad *vs* almost the same length as broad; dorsal ridge in stoma located anterior to pharyngeal collar *vs* at level of pharyngeal collar; female tail <7 anal body diam. long and uniformly conoid *vs* >7 anal body diam. long and with filiform tip; male with first three subventral genital papillae (GP1-3) equidistant in spacing *vs* GP1 >3× the distance to GP2 than between GP2 and GP3; cloaca covered by trapezoidal flap with single peg-like papilla at base and bifurcate distal edge *vs* a single peg-like papilla anterior to level of cloacal aperture and two small ventral peg-like papillae immediately posterior to cloacal aperture (although the two small ventral peg-like papillae might have been a misinterpretation of a bifurcate distal edge on a cloacal flap); and two pairs of terminal genital papillae (GP6-7) *vs* three pairs (GP6-8).

It is unclear whether the sexual dimorphism observed in the deirids of *M. byersi* n. sp. is an important autapomorphy or a character that is present in other *Myolaimus* species but not reported.

Molecular profiles

The DNA sequences of near full length SSU and two non-contiguous fragments of the LSU of *M. byersi* n. sp. are available in the GenBank database with accession numbers AB478627 (this study), DQ145643 and DQ145691 (Nadler *et al*., 2006), respectively.

TEM ultrastructure (Figs 7-11)

These are the first ultrastructural observations of the baggy cuticle, stoma, sensory system and sperm of *Myolaimus*. In all regions where the cuticle was observed with apparent duplicature, it had an intact basal layer attached to the epidermis while the cortical and epicuticle were separated by a disassociated median layer (Figs 3; 4; 6A; 7B; 11A). Thus, the baggy or swollen cuticular appearance in adults is not due to a retained or extra cuticle as some have suggested. This was not confirmed by TEM for dauers, but seems a reasonable hypothesis given the appearance of the cuticle of the dauer stage.

The oral aperture of *M. byersi* n. sp. is triradiate while the buccal cavity varies in cross-section from triradiate at its anterior and posterior ends to complex shapes with bilateral symmetry in between. In lateral view, the posterior edge of the dorsal cheilostomatal wall and the

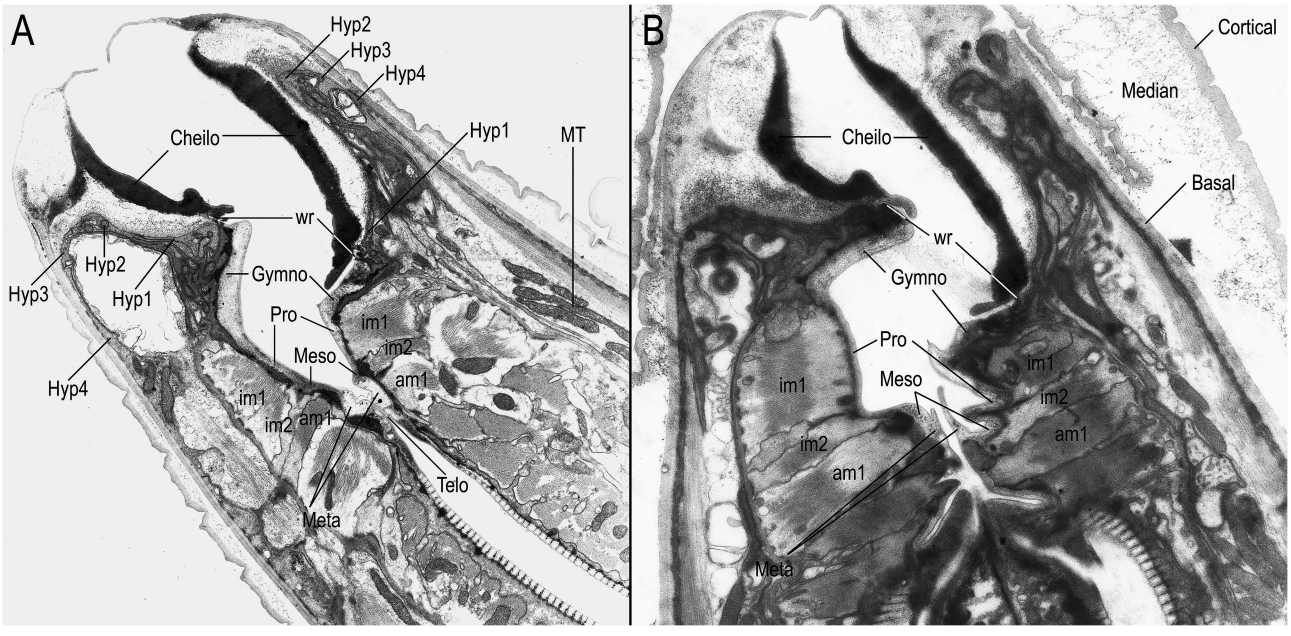

Fig. 7. *Near sagittal transmission electron micrographs of anterior region of* Myolaimus byersi *n. sp. A: Female; B: Male. Abbreviations: am1 = anterior adradial muscle cell lining stoma; am2 = posterior adradial muscle cell lining stoma; Basal = basal zone of cuticle; Cheilo = cheilostom; Cortical = cortical zone of cuticle; Gymno = gymnostom; Hyp1, Hyp2, Hyp3, Hyp4 = cheilostom epidermal syncytia 1-4, respectively; im1 = anterior interradial muscle cell; im2 = posterior interradial muscle cell; Median = median zone of cuticle; Meso = mesostegostom; Meta = metastegostom; MT = mitochondria; Pro = prostegostom; Telo = telostegostom; wr = membrane wedge ring.*

anterior edge of the gymnostom almost meet at a straight angle, appearing somewhat like a composite dorsal ridge or tooth. The non-segmented cheilostom is anisomorphic in lateral view with the dorsal wall only about two-thirds as long as the walls of its subventral sectors. The lining of the cheilostom is two-layered with an electron dense surface layer surrounded by an electron lucent peripheral layer, both visible in cross-sections and in lateral view. Anteriorly, the electron dense layer appears to originate and share affinities with the basal layer of the cuticle whereas the origin of the electron lucent layer is peripheral to the electron dense layer and appears to emerge from the cephalic cytoskeleton. In the posterior dorsal wall of the cheilostom the translucent layer ends first, leaving an electron dense cheilostomatal rim that projects obliquely posteriad towards the anterior oblique edge of the gymnostom.

The cheilostom is lined by four epidermal syncytia in a series of sequential toroids (= rings). Epidermal syncytia are distinct from the arcade cells lining the gymnostom in having a more electron lucent cytoplasm. The innermost syncytium is thin and borders the anterior arcade cell of the gymnostom; it has (at least) one ventral and two dorsolateral posterior processes. Anterior to this is a syncytium with a comparatively prominent toroid that lines the most anterior stomatal cuticle. The syncytium itself has (at least) one ventral process (other possible processes are unclear). A third syncytium, along with the second syncytium, also lines the most anterior stomatal cuticle. This syncytium has pockets in which internal receptor neurons are embedded and has (at least) two dorsal posterior extensions. A fourth syncytium lines the outermost part of the cheilostom and has (at least) one dorsal and one ventral and two lateral posterior extensions. Socket cells of cuticular sensilla attach to the cuticle between pairs of epidermal syncytia – between the second and third syncytia are the socket cells of the inner labial syncytia and between the third and fourth are socket cells of the outer labial and cephalic sensilla. The amphid socket cell is anchored, at least anteriorly, in the fourth syncytium.

Myolaimus byersi n. sp. possesses an anisomorphic gymnostom of which the dorsal sector is more than twice as long as the subventral sectors. In sagittal sections,

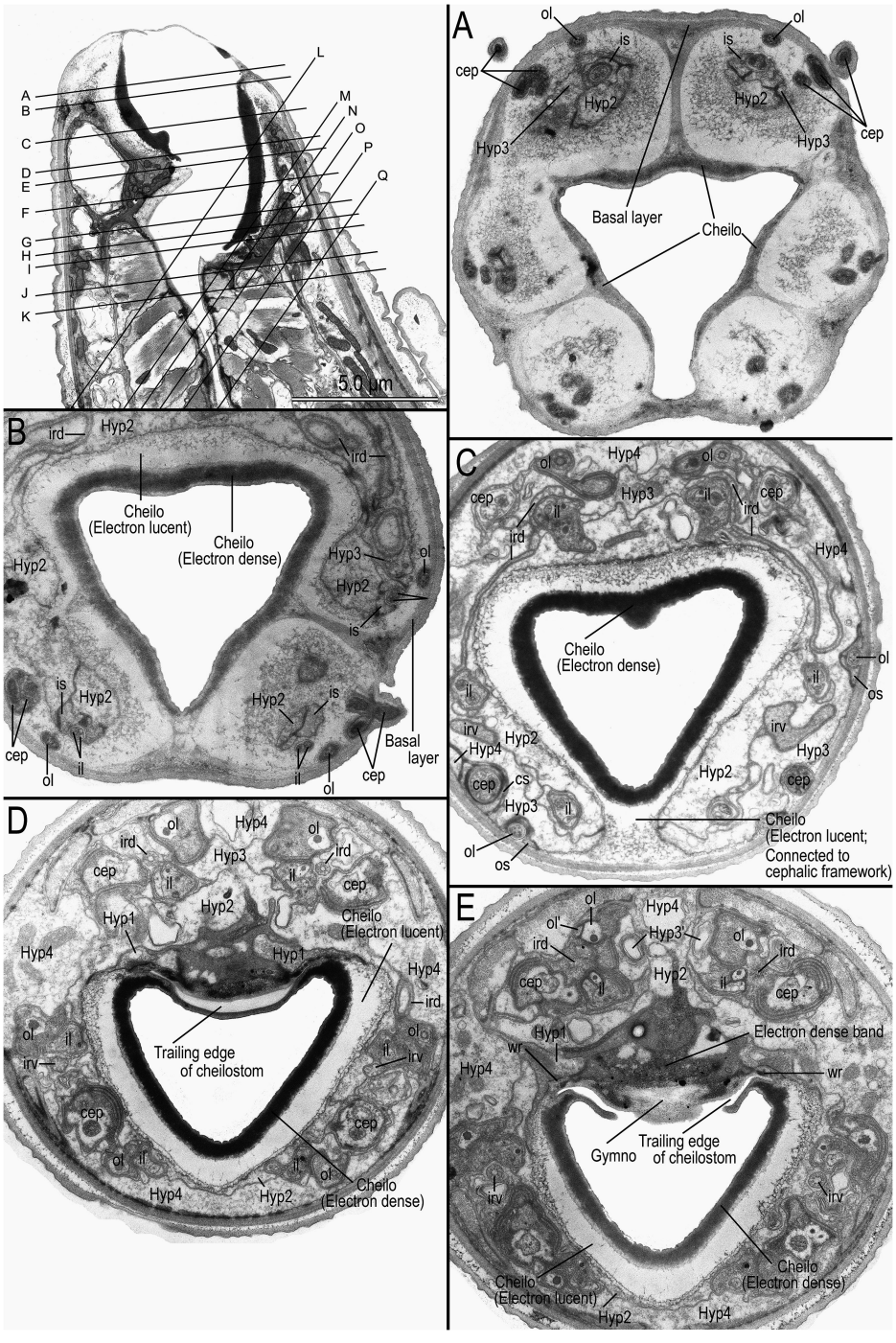

Fig. 8. *Near sagittal transmission electron micrograph of anterior region of* Myolaimus byersi *n. sp. female with locations of transverse sections for Figs 8A-E; 9F-K and 10L-Q. A-E: Male. Abbreviations: cep = cephalic dendrite(s); cs = cephalic socket cell; Hyp3' = posterior process of Hyp3; il = inner labial dendrite(s); is = inner labial socket cell; ird = subdorsal ciliated internal receptor; irv = ventrolateral ciliated internal receptor; ol = outer labial dendrite; ol' = bare, internal outer labial dendrite; os = outer labial socket cell (see Fig. 7 for abbreviations to other labels). (The section location bar labelled A is* ca. *8 µm long.)*

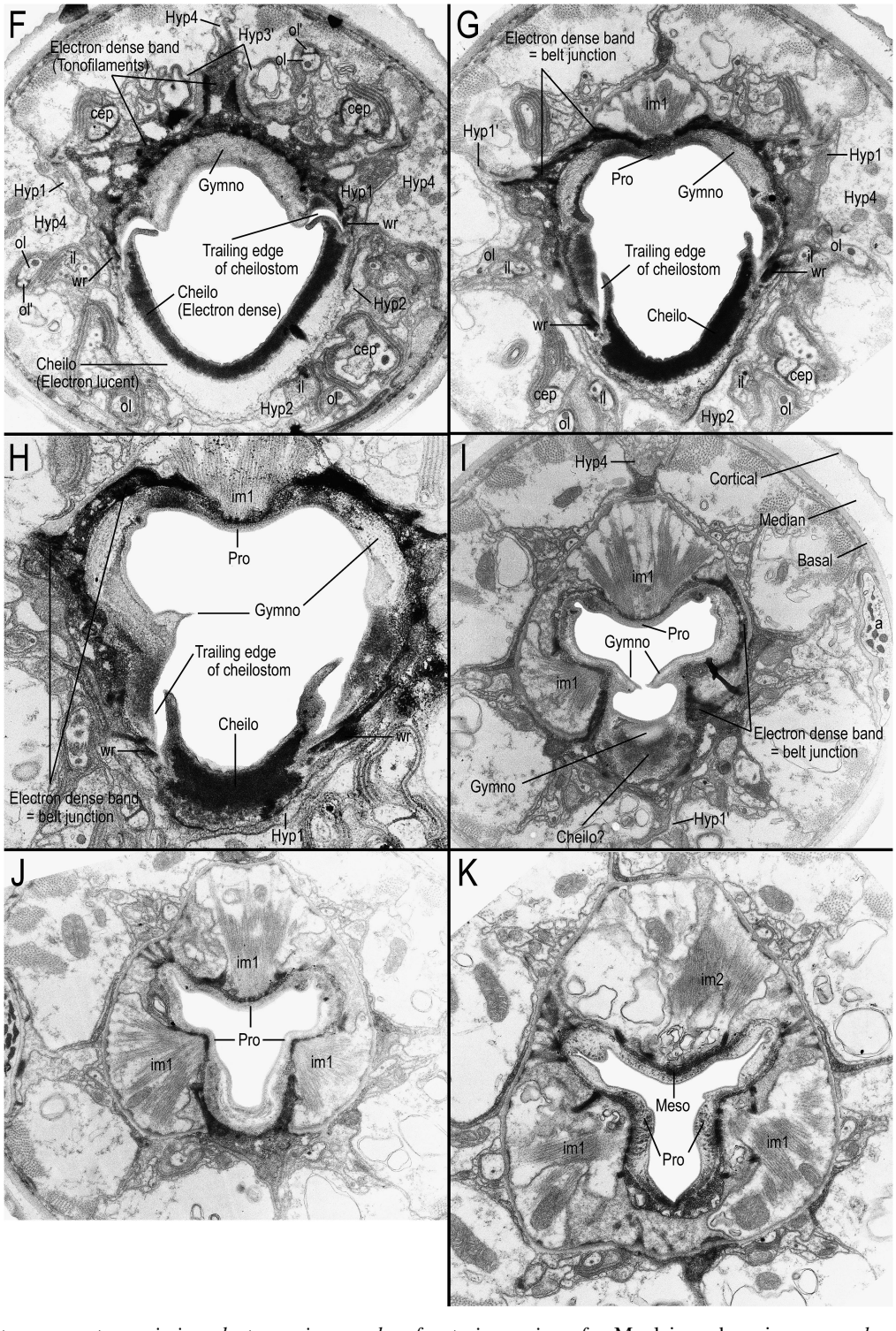

Fig. 9. *Near transverse transmission electron micrographs of anterior region of a* Myolaimus byersi *n. sp. male. Abbreviations: a = amphid; Hyp1' = posterior process of Hyp1 (see Fig. 8 for relative location and scale of sections F-K and Figs 7, 8 for abbreviations to other labels).*

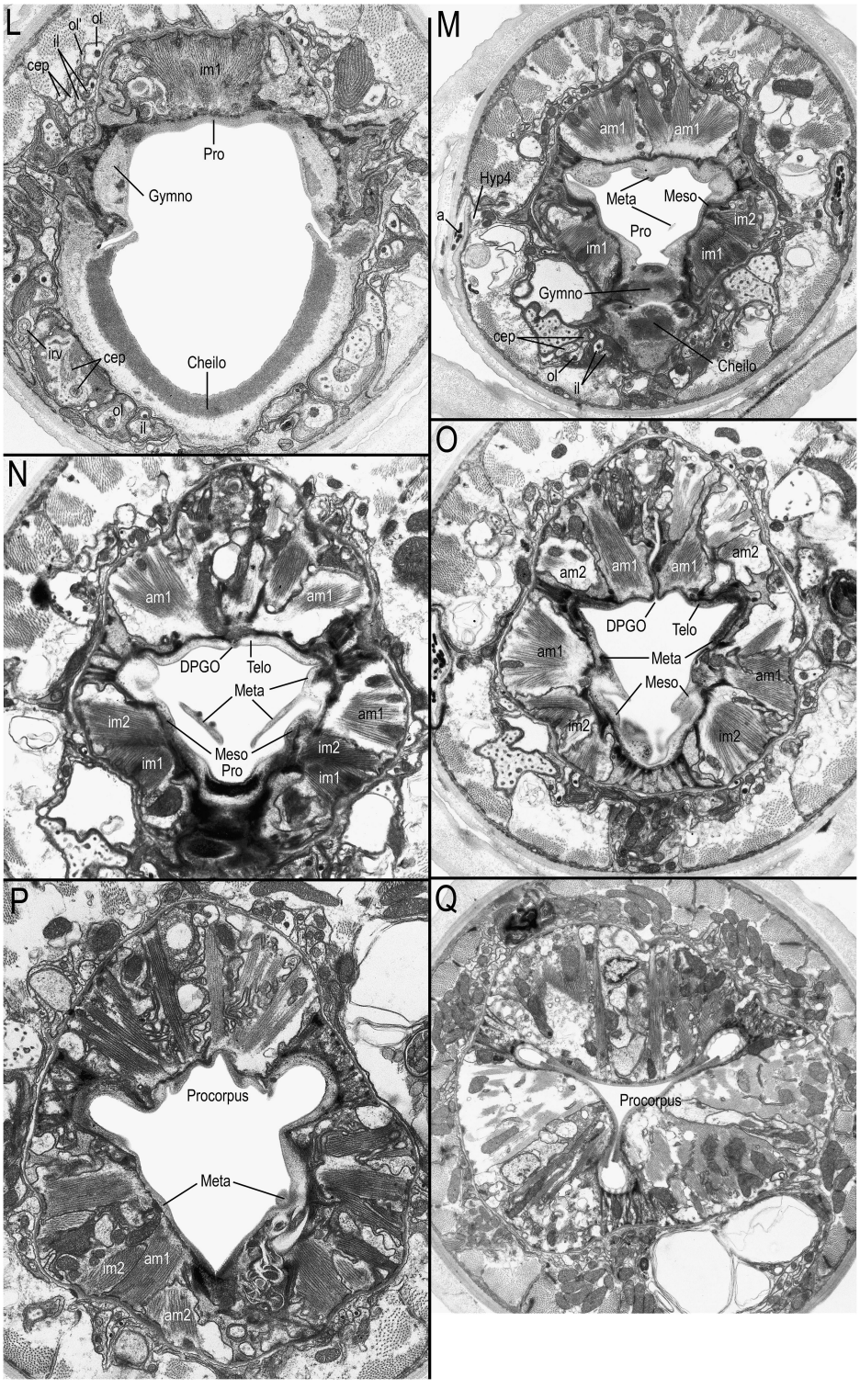

Fig. 10. *Oblique transverse transmission electron micrographs of anterior region of a* Myolaimus byersi *n. sp. female. Abbreviations: DPGO = dorsal pharyngeal gland orifice (see Fig. 8 for relative location and scale of sections L-Q and Figs 7-9 for abbreviations).*

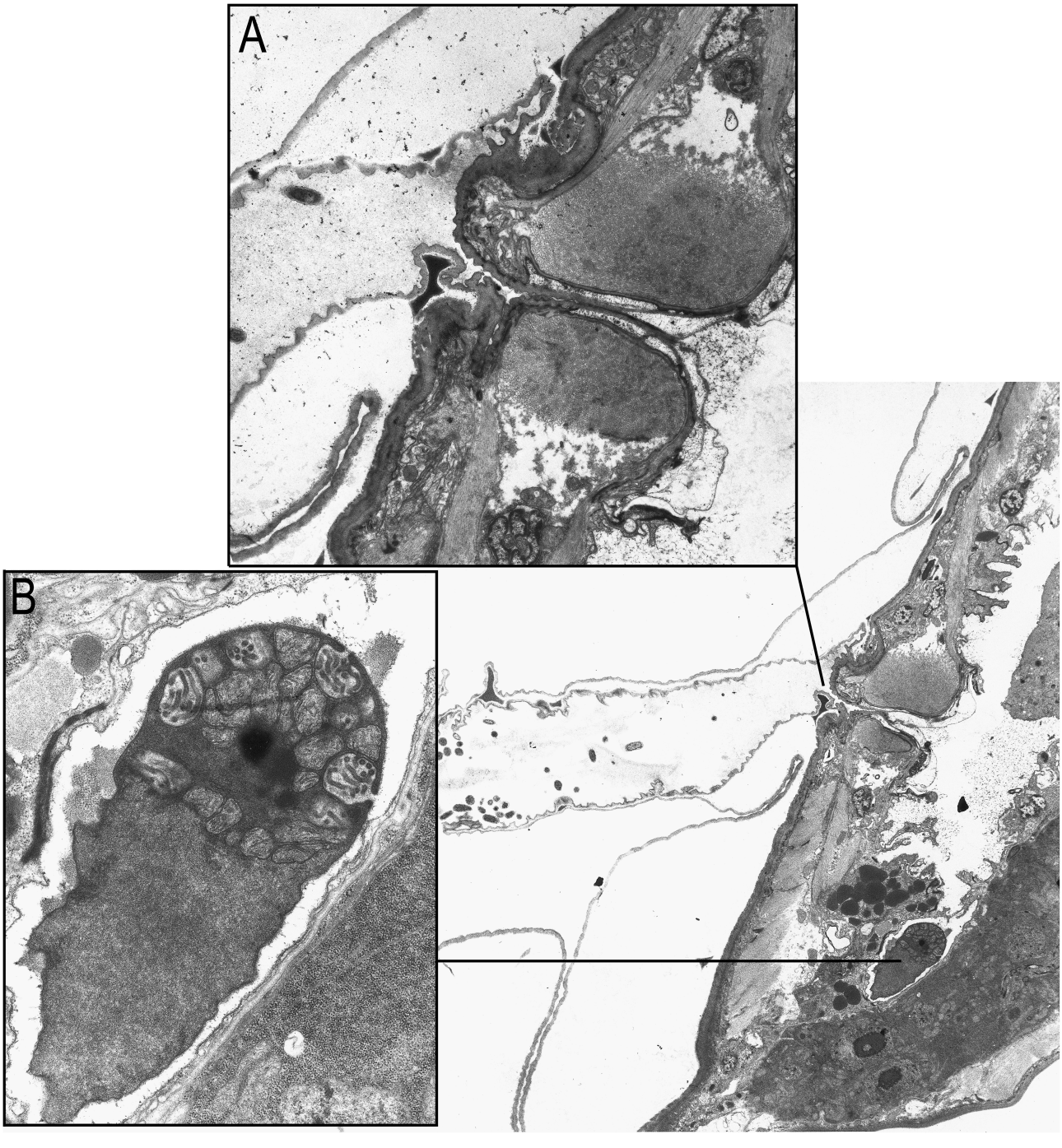

Fig. 11. *Near sagittal transmission electron micrograph of mid-body of a* Myolaimus byersi *n. sp. female in copulation with a male. A: Close-up of vagina and vulva; B: Close-up of mature sperm cell in female reproductive tract.*

a distinct gap occurs all along the posterior rim of the cheilostom cuticle and the anterior cuticle of the gymnostom, with a membrane junction inserting as a wedge in between both types of cuticle and reaching the edge of the buccal lumen at the bottom of the gap. Two more membrane junctions impinge on the gymnostom cuticle but do

not traverse it, corresponding to two surrounding sets of arcade cells. In transverse sections no membrane junctions are evident within either arcade cell ring, suggesting that each ring is a syncytium. However, the different proportions of the dorsal and subventral sectors of the gymnostom render the exact position of each arcade ring rather difficult to trace, especially in the subventral sectors. The posterior edge of the gymnostom is surrounded by a transverse ring of electron dense material. The basal lamina of the pharynx curves towards the buccal cavity at this point and contacts the ring of electron dense material without directly impinging on the buccal cuticle. The prostegostom is also anisomorphic in lateral and ventral views. The transition from gymnostom to prostegostom and then to mesostegostom is spatially complex in cross-section because of the different proportions of the dorsal sector *vs* both subventral sectors. The buccal cavity assumes a pronouncedly bilateral symmetry at this level with relatively simple subdorsal radii *vs* a much wider and deeper ventral radius, the latter flanked by paired oblique ridges where the posteriorly extended ventral cheilostomatal cuticle is succeeded first by a very short stretch of gymnostomatal lining and then by stegostomatal cuticle.

The prostegostom and mesostegostom are associated with the anterior end of the respective im1 and im2 muscle cells, of which there is one in each interradial sector or three cells all around. The dorsal sectors of the pro- and mesostegostom and their associated muscles are noticeably longer than their subventral counterparts. The metastegostom is associated with two adradial am1 muscle cells and one anteriorly directed triangular flap or denticle in each sector. The two subventral denticles appear to be somewhat larger and more posteriorly placed than the dorsal denticle, although this is difficult to determine exactly because of the dorso-subventral anisomorphy of the buccal sectors. The dorsal pharyngeal gland orifice (DPGO) opens just posterior to the dorsal metastegostom denticle at the edge of the telostegostom. The telostegostom appears as an inverted triangle in cross-section and each side is associated with two adradial am2 muscle cells. A single neuronal process touches the dorsal lining of the stegostom in between the dorsal denticle and the DPGO. Each subventral sector also has a neuronal process reaching the cuticle in between both am1 cells and both am2 cells and at the junction of the meta- and telostegostom. One epithelial cell extends across the tip of each radius of the entire stegostom, transversely separating the three interradial muscle cells of the pro- and mesostegostom, respectively, as well as separating the three pairs of adradial muscle cells in meta- and telostegostom consecutively.

The anterior sensory system of *M. byersi* n. sp. males and females includes six inner labial, six outer labial and four cephalic sensilla, in addition to the two amphids. Each inner labial sensillum has two ciliated dendrites exiting the cuticular duct of the socket cell. The lateral and quadrant outer labial sensilla each have one ciliated dendrite that terminates in a corresponding labial seta. In addition, each lateral and quadrant outer labial sensillum has a thin, bare (= non-ciliated) dendrite that enters the sensory channel of the sheath cell shortly before terminating, the two dendrites of each outer labial sensillum connecting to each other by gap junctions within the sheath cell. Cephalic sensilla each have two ciliated dendrites, one running within its respective cephalic seta and one terminating in the lip. Two classes of ciliated internal receptors, each comprising a pair of dendrites, were also identified in the anterior of the nematode. One pair of subdorsal receptors has large basal bodies and expansive termini. Distally (anteriorly) the cilia flatten and lie against the lateral margins of the dorsal inner labial support cells. The cilia have flat, subdorsal and lateral extensions that wrap around neighbouring cells, possibly epidermis or the support cells of cuticular sensilla. Ciliated dendrites of a second class are axially ventrolateral and have large, swollen termini embedded in an epidermal syncytium.

As revealed by TEM, sperm in the oviduct of a mated female of *M. byersi* n. sp. is nearly identical to the bipolar cell described for *C. elegans* (Kimble & Ward, 1988; Yushin & Malakhov, 2004). The rounded main cell body (MCB) contains an electron dense nucleus (without a nuclear envelope), mitochondria and membranous organelles (MO) that are filled with "internal finger-like projections" that have fused with the plasmalemma (Kimble & Ward, 1988; Yushin & Malakhov, 2004). The anteriormost pseudopod appears less electron-dense and fibrous bodies were not observed in the mature sperm.

Studies on embryonic development

In the sequence of early cell divisions, *M. byersi* n. sp. was most similar to *P. equorum* (Table 2) with only a switch between the P3 and E cell divisions. It was next closest to *C. elegans* with a switch between the P2 and EMS cell divisions and then a delay of the E cell division until after the $^{8}AB^{16}$ division (Table 2). *Panagrolaimus* sp. and *A. nanus* appeared derived relative to *M. byersi* n. sp. with many changes starting with the second cell division.

Table 2. *Sequence of early cell divisions in five nematode species including* Myolaimus byersi *n. sp.*

Parascaris equorum (clade 8)	*Caenorhabditis elegans* (clade 9)	*Panagrolaimus* sp. (clade 10)	*Acrobeloides nanus* (clade 11)	*Myolaimus byersi* n. sp. (clade 9)
P0	P0	P0	P0	P0
AB	AB	P1	P1	AB
P1	P1	AB	P2	P1
^{2}AB^{4}	^{2}AB^{4}	P2	AB	^{2}AB^{4}
P2	EMS	^{2}AB^{4}	P3	P2
EMS	P2	EMS	^{2}AB^{4}	EMS
^{4}AB^{8}	^{4}AB^{8}	P3	EMS	^{4}AB^{8}
MS	MS	^{4}AB^{8}	^{4}AB^{8}	MS
C	E	MS	MS	C
E	C	E	E	P3
^{8}AB^{16}	P3	C	C	^{8}AB^{16}
P3	^{8}AB^{16}	^{8}AB^{16}	^{8}AB^{16}	E

Clades are as listed according to De Ley and Blaxter (2002).

Table 3. *Developmental characters during early embryogenesis in five selected nematode species including* Myolaimus byersi *n. sp.*

Character	*Parascaris equorum* (clade 8)	*Caenorhabditis elegans* (clade 9)	*Panagrolaimus* sp. (clade 10)	*Acrobeloides nanus* (clade 11)	*Myolaimus byersi* n. sp. (clade 9)
Smooth egg shell	+	+	+	+	–
Pronuclei migration	?	+	+	–	+
1st PB extruded at anterior pole	–	+	–	–	–
Early nucleoli	?	–	+	+	+
T-like 4-cell stage	+	–	–	–	+
l-r asymmetry ABs	+	+	+	+	+
Nuclei adjacent E/P3	?	+	+	–	+
Polarity reversal P2	+	+	+	–	+

Clades are as listed according to De Ley and Blaxter (2002).

Table 3 summarises some developmental characters during embryogenesis from the same group of nematodes. The only potentially apomorphic character was the possession of a spiny egg shell relative to the others that had a smooth egg shell. However, plectids have spiny egg shells, so this could actually be a plesiomorphy. *Myolaimus byersi* n. sp. shares a T-like four-cell stage only with *P. equorum*, but shares the character of the first polar body being extruded at the anterior pole with all of the other nematodes studied, except *C. elegans*. The left-right asymmetry of the AB cells is an apparent ancestral character shared by all of the nematodes including *M. byersi* n. sp. (Table 3). *Acrobeloides nanus* appears derived compared with the rest of the nematodes studied in the loss of pronuclei migration, a lack of nuclei being present adjacent to E/P3 and the lack of a polarity reversal of P2 (Table 3).

Insect association studies

Many different invertebrates were collected and dissected from the decomposing palm tissue, including all stages of *M. hemipterus*, rove beetles (Staphylinidae), earwigs (Dermaptera), woodroaches and millipedes, but only the crane fly *L.* (*R.*) *schwarzi* was observed to be associated with dauers that were confirmed through culturing to be *M. byersi* n. sp. Of the 73 *L. schwarzi* adults dissected over the course of the caged tissue study, 33% were observed with dauers of *M. byersi* n. sp. Dauers were recovered from the intersegmental abdominal folds of 42% of male *L. schwarzi* ($n = 48$; 73 ± 86 (2-296) dauers

per host; range) and 16% of females (n = 25; 54 ± 91 (1-190). Five *L. schwarzi* larvae were extracted from nematode infested decomposing palm tissue for observation and dissection. Of these, none was found to be internally infested with dauers, an average of about 50 dauers were observed in the webbing surrounding each larva and 25 dauers were associated externally on each larva. Of the five pupae that were extracted and observed as above, none was found to be internally infested with dauers, an average of 130 dauers were observed in the webbing surrounding each pupa and 65 dauers were associated externally on each pupa. The larvae and pupae of *L. schwarzi* are quite mobile and the dauers of *M. byersi* n. sp. moved quickly to maintain their external association with their carrier. Adult flies that had been histologically sectioned to observe the association showed that most nematodes were washed out from the intersegmental folds during the many histological steps. However, we did observe several dauers in cross-sections and there appeared to be no involvement other than being free in the fold. This argues for a relatively host specific and synchronised external phoretic association.

Except for the baggy cuticle (Fig. 2), the dauer stage appeared very similar in morphology to panagrolaimid dauers that have occasionally been described in earlier literature, such as *Panagrolaimus rigidus* (Körner, 1954).

Discussion

The ultrastructure of the sperm is a synapomorphic character that *M. byersi* n. sp. shares with *C. elegans* and supports the inference that *Myolaimus* belongs to the Rhabditida clade *sensu lato* (De Ley & Blaxter, 2002). Inferences from molecular sequence data from LSU suggest that *Myolaimus* sits near the deepest known root of the 'Rhabditida'; *i.e.*, that it split off from the same lineage as the cephalobs/panagrolaims/tylenchids/aphelenchoids/rhabditids/diplogastrids and has remained distinct since that time (Nadler *et al.*, 2006). The embryogenesis data presented herein (Tables 2, 3) generally support the LSU inferences. Thus, the apomorphies of baggy cuticle, a tube-like, cuticular vulval sac and an aspiculate mating strategy may be quite ancient in *Myolaimus* and also in the genus *Deleyia* Holovachov & Boström, 2006 (Holovachov & Boström, 2006). However, molecular sequence data are needed from *Deleyia* to resolve better the relationship between these two genera.

In most *Myolaimus* species described thus far, stomatal structures were not described in great detail, although the general stoma was described as a variably-shaped cylinder with a large to medium-sized dorsal tooth, sometimes with two subventral teeth. Andrássy (1959) drew a segmented cheilostom and imposed classical rhabditid morphology and nomenclature on what he described for the stoma of *M. amititiae*. Yet, the pharyngeal collar only engulfed the posteriormost region of that stoma, suggesting that what Andrássy called cheilo-, pro- and mesostom were, in fact, only cheilostom and that the stoma was similar to what we describe for *M. byersi* n. sp., except that it was longer and much more isomorphic, both in terms of the stomatal and anterior pharyngeal components. Andrássy (2005) drew the stoma of *M. tepidus* similarly to *M. amititiae* except that the stegostomatal region was significantly reduced in comparison. Ali *et al.* (1970) reported that in *M. indicus* the cheilostom, prostom (= gymnostom) and mesostom (= prostegostom) were fused to form a broad triangular chamber with the pharyngeal collar extending dorsally up to the base of the mesostom and the metastom with a large ventrally curved dorsal tooth. Hnatewytsch (1929) depicted a similar stoma for *M. maupasi* which appeared analogous to a diplogastrid stoma. The stoma of *M. stammeri* was depicted as more squat than other species of *Myolaimus* and with a large dorsal tooth and two subventral teeth ensheathed by the pharyngeal collar, suggesting compression in some components relative to *M. byersi* n. sp. (Hirschmann, 1952). The stoma of *M. rahmi* was drawn longer and thinner than all other described *Myolaimus* (Rahm, 1928), but the relative position of the dorsal ridge and the pharyngeal collar suggest strong affinities to *M. byersi* n. sp. The stoma of *M. dendrodipnis* was drawn slightly shorter than *M. rahmi* (Paesler, 1956), but was similar in general morphology to what we have observed for *M. byersi* n. sp.

Comparisons of the ultrastructure of the stoma from bacterivorous and parasitic representatives from Rhabditida clades (*Panagrolaimus superbus*, *Zeldia punctata*, *Caenorhabditis elegans*, *Caenorhabditis* sp. PS-1010, *Heterorhabditis bacteriophora*, rhabditid sp., *Acrostichus halicti* and *Parasitodiplogaster laevigata* (Van de Velde *et al*., 1994; De Ley *et al.*, 1995; Baldwin *et al.*, 1997a, b; Giblin-Davis *et al.*, 2006)) demonstrate plasticity in the derivation of the stoma. *Myolaimus* is no exception with a large anisomorphic and partly triradiate stomatal chamber which, in contrast to others, is primarily composed of the cheilostom (derived from the epidermis). Unlike the reverse condition commonly observed in other Rhabditida, the trailing edge of the cheilostom projects obliquely posteriad into the buccal cavity and partly overhangs the

gymnostom cuticle. However, as with all other Rhabditida studied ultrastructurally thus far, cheilostom and gymnostom cuticle in *Myolaimus* are fully separated from one another by a membrane wedge ring inserting between both and reaching the edge of the buccal lumen. Multiple ridge-like features arise from the complex combination of anisomorphy of successive buccal regions with change from triradiate to bilateral symmetry and with overlapping edges of cheilostom and gymnostom cuticle. Depending on angle of view and condition of preservation, these ridges could have been misinterpreted as teeth in previous descriptions. There are genuine triangular denticles in the stegostom, however, so these could also explain some of the past reports of subventral teeth. This contrasts with the dorsoventral isomorphy of many other rhabditids that have been studied ultrastructurally, such as *C. elegans*, *Caenorhabditis* sp. PS-1010, *H. bacteriophora*, *Pelodera* sp. or panagrolaims such as *P. superbus*, or cephalobs such as *Acrobeloides* sp. (Van de Velde *et al*., 1994; De Ley *et al.*, 1995; Baldwin *et al.*, 1997a) and is more similar in appearance to the diplogastrids such as *A. halicti* and *P. laevigata* (Baldwin *et al.*, 1997b; Giblin-Davis *et al.*, 2006). Interestingly, in the Rhabditina, the cylindrical or prismatic stoma tube results from the elongation of different regions in different taxa, *e.g.*, gymnostom in *Pelodera* sp. *vs* a more evenly sized gymnostom, pro- and mesostegostom or mesostegostom as in *C. elegans* and *Heterorhabditis* (De Ley *et al.*, 1995). The presence of one triangular flap or denticle in each sector of the metastegostom is similar to the condition of many Rhabditina, including *C. elegans* (De Ley *et al.*, 1995; Baldwin *et al.*, 1997a).

The associated anterior pharyngeal muscles of the stegostom follow the pattern of the cephalobs and panagrolaims within the pharyngeal collar, the prostegostom and mesostegostom being successively associated with a first and second ring of three interradial muscles each (Fig. 12). The metastegostom and telostegostom are successively associated with a third and fourth ring of six adradial muscles layered like a cake (Fig. 12).

If *Myolaimus* is indeed one of the earliest branches within the phylogeny of Rhabditida and Myolaimina are an outgroup of the splits within and between Clades IV and V (Blaxter *et al.*, 1998), then the expanded dorsal sector of diplogastrids is probably not an autapomorphy, the presence of three denticles in Rhabditina is not an autapomorphy and the $3 + 3 + 6 + 6$ arrangement of stegostomatal muscle cells in cephalobs/panagrolaims is not an autapomorphy. It is the massive anisomorphic cheilostom and oddly anisomorphic gymnostom that appear apomorphic in *Myolaimus* relative to other nematodes in the Rhabditina, Cephalobina and Panagrolaimidae.

Limited TEM observation reveals general conservation of epidermal syncytia in *M. byersi* n. sp. with respect to several taxa in Rhabditida. As in *C. elegans*, for which the anterior epidermis has been fully reconstructed (White, 1988), the cheilostom of *M. byersi* n. sp. includes four layers of epidermal syncytia. Epidermal syncytia are thus hypothesised to be, from the gymnostom to the body wall, Hyp1 through Hyp4. Putative homologies with *C. elegans*, as well as other Rhabditida representatives *Acrobeles complexus* (Bumbarger *et al.*, 2006) and *Aphelenchus avenae* (Ragsdale *et al*., 2008), are corroborated by the spatial relationships of epidermal syncytia to cells of the anterior sensory system, which are highly conserved within Rhabditida. The positions of the inner labial socket cells between Hyp2 and Hyp3 homologues and those of outer labial and cephalic socket cells between Hyp3 and Hyp4, are conserved with respect to all three examined Rhabditida. The apparent association of the amphid socket cell with only Hyp4 in the cheilostom is unique to *M. byersi* n. sp. Also conserved between *M. byersi* n. sp. and Rhabditida ingroups are the association of internal receptor cilia with a particular epidermal homologue, lending support to that syncytium as Hyp3. Positions of posterior processes of cheilostom epidermal syncytia, which presumably lead to nuclei (possibly excepting the lateral processes of Hyp4), are consistent with putative homologues in Rhabditida representatives.

Putative homologies of the anterior sensory system with respect to Rhabditida polarise corresponding characters distinct between major clades of Rhabditida. Comparisons can be made to those nematodes in which the anterior sensory cells have been reconstructed: *C. elegans* (Ward *et al*., 1975; White *et al.*, 1986) in Clade V and *Acrobeles complexus* (Bumbarger *et al.*, 2007) and *Aphelenchus avenae* (Ragsdale *et al*., 2009) in Clade IV. Characters that are apparently symplesiomorphic in Clade IV and *M. byersi* n sp. relative to Clade V are: the presence of two outer labial dendrites, one of which is bare and terminates within the sheath cell and the presence of two cephalic dendrites in the female. Conserved in both *M. byersi* n sp. and all three Rhabditida representatives is the presence of two ciliated inner labial dendrites. In *M. byersi* n. sp., two classes of prominent, ciliated internal receptors, a subdorsal pair and a ventrolateral pair, are hypothesised to be homologues of the FLP and BAG dendrites of *C. elegans*, respectively. The terminus of putative FLP in *M. byersi* is similar to FLP of *C. elegans* in forming a

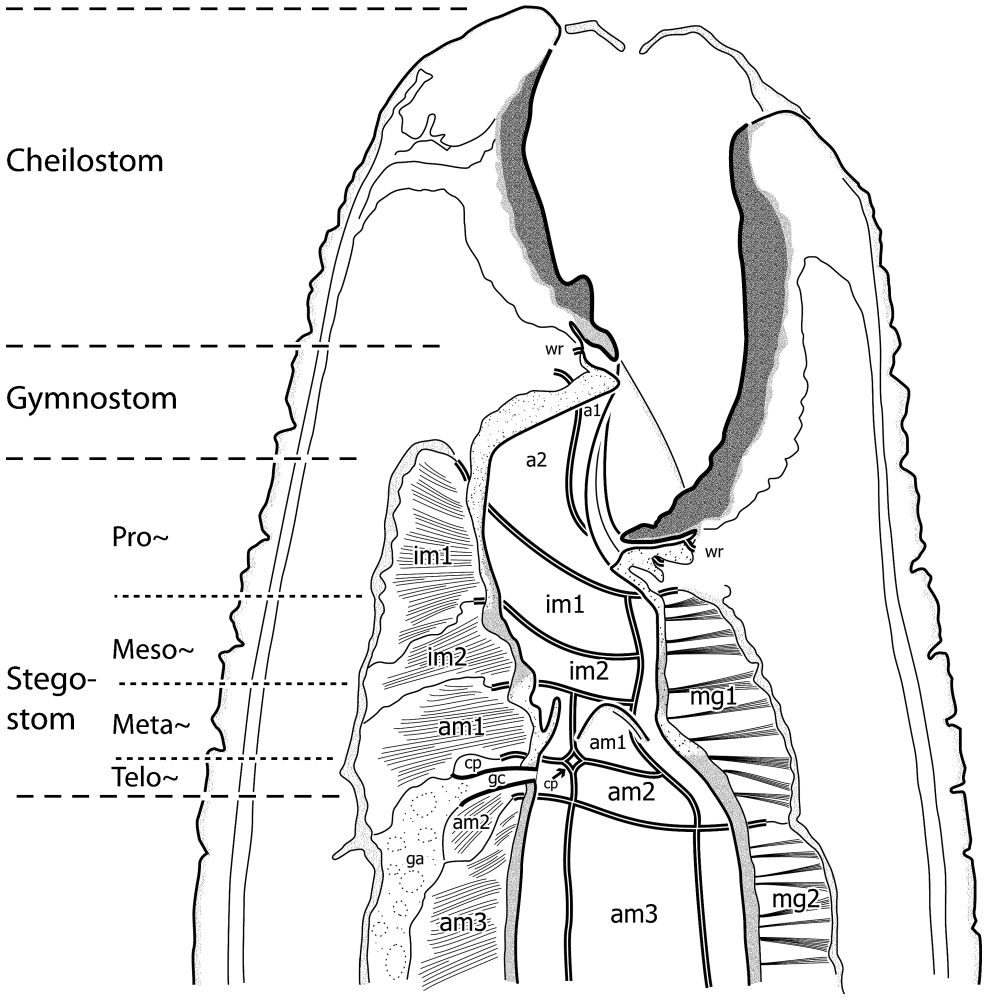

Fig. 12. *Cuticular and cellular architecture of stoma in* Myolaimus byersi *n. sp., based on two nearly complete series of transverse sections and two partial series of longitudinal sections. Bold double lines represent the delineation of cell junctions underlying the left-subventral cuticle of the buccal lining. Abbreviations: a1 = anterior arcade syncytium; a2 = posterior arcade syncytium; am1 = anterior adradial muscle cell lining stoma; am2 = posterior adradial muscle cell lining stoma; am3 = anterior adradial muscle cell lining corpus; cp = tip of neuronal cell process; im1 = anterior interradial muscle cell; im2 = posterior interradial muscle cell; ga = dorsal gland ampulla; gc = dorsal gland canal; mg1 = marginal cell lining the tip of stoma radius; mg2 = marginal cell lining the tip of corpus radius; wr = membrane wedge ring separating cheilostom cuticle from gymnostom cuticle.*

flat 'flap' that wraps around neighbouring cells, although the expanse of the terminus seems greater in *M. byersi* n sp., thereby contrasting with the simple, bare FLP dendrite described in Clade IV nematodes. As in all three examined Rhabditida, putative BAG in *M. byersi* n. sp. has a prominent cilium and an enlarged terminus, although in *M. byersi* n. sp. it does not wrap around epidermis but is instead swollen and simply embedded within Hyp3. The essentially unbranched termini of proposed BAG homologues in *M. byersi* n. sp. and *C. elegans* are both limited in expanse compared to those in Clade IV taxa, in which the multilamellar BAG terminus extends throughout the cheilostom.

An apomorphy in *M. byersi* n. sp. includes the appearance of the body cuticle which can form a bag-like sheath that extends up to and around natural openings. This is a feature that is shared with nematodes such as *Deleyia* and several other genera (Holovachov & Boström, 2006). Based on our TEM observations, this phenomenon in *Myolaimus* is due to a dissociation or dissolution of the me-

dian layer of the cuticle allowing the basal and cortical layers to move relatively freely over the body. The adaptive purpose of this is unknown, but may be important for defence against nematode-trapping fungi and as a mechanism of avoidance or deterrence of invasion by pathogens or body wall penetration by predators.

The entire mating strategy is apomorphic with the loss of gubernaculum and spicules, formation of a bursa-like tail, stout, finger-like caudal papillae, heavily cuticularised cloaca (that in *M. byersi* n. sp. extends to the tail knob with an autapomorphic cloacal flap) and a highly derived mating strategy that apparently eliminated the functional need for a gubernaculum and spicules and which involves a spermatophore ejaculate (Fürst von Lieven *et al.*, 2005). There are the corresponding functional apomorphies in the female involving an elephant trunk-like vulval sac to accommodate the spicule-less male copulatory system and spermatophore. Yet, sperm ultrastructure appears highly conserved.

Other aspects that appear highly conserved include the formation of dauers and a derived association with an insect in a relatively host-specific manner. Also, with regard to the anterior region of both sexes, the apparent retention of triradiate (hexaradiate in some regions) rings throughout all components of the stoma, DPGO location just posterior to the junction between the meta and telostegostom, amphid shape and position similar to the conserved pattern not unlike *Plectus* with the presence of setiform labial and cephalic sensillae that exhibit no sexual dimorphism. The Myolaimidae have seven GP and phasmids which are positioned posteriorly between the first five papillae and the last two with a pattern more analogous to cephalobids which possess 7-8 GP and phasmids situated anteriorly to the three posteriormost papillae, with a lot of variability (but the phasmids are not terminal as in the case of the panagrolaims) (Kiontke & Sudhaus, 2000). *Myolaimus stammeri* and *M. amititiae* were originally described with eight GP inclusive of three terminal papillae. This number was retained by Andrássy (1984) for *M. stammeri* but was reduced to two for *M. amititiae*. In 2005, two terminal papillae were reported for both species (Andrássy, 2005).

Myolaimus has a conserved 'Cephalobina' (Clade IV) final vulval fate pattern of $2^\circ - 1^\circ - 1^\circ - 2^\circ$ *vs* the $2^\circ - 1^\circ - 2^\circ$ of rhabditids and dipolgastrids (Clade V) (Felix *et al*., 2000; Sommer, 2005). It is unclear how the centrally positioned but monodelphic vulva of *Myolaimus* is induced, but loss of the posterior branch is not because of a programmed cell death as it is in *Panagrolaimus*, *Halicephalobus* and *Cephalobus* (Felix *et al*., 2000; Sommer, 2005). Thus, *Myolaimus* appears to have been on an independent, non-coalescing trajectory for a long time, allowing it to retain and manifest some highly conserved characters while developing some surprisingly unique ones. However, much more developmental, ultrastructural and molecular work is needed from Myolaimina and related nematodes for developing hypotheses about the evolution of this very interesting nematode lineage.

Acknowledgements

Special thanks to Dr George Byers at the University of Kansas for identification of *L.* (*R.*) *schwarzi* and for sharing information concerning the biology of crane flies and their parasites and predators, Dr Weimin Ye and Dr W. Kelley Thomas for help with molecular samples, Dr Jim Baldwin for early discussions concerning stomatal ultrastructure and Ms Verena Bärmann, Dr Walter Sudhaus and Dr Alex Fürst von Lieven for advance communication concerning their upcoming *Myolaimus* revision. This study was supported in part by awards from the National Science Foundation (NSF) Biotic Surveys and Inventories, Partnerships for Enhancing Expertise in Taxonomy and Tree of Life programs (DEB-0450537; DEB-0640807; DEB-0731516; DEB-0228692) and a USDA Special Grant in Tropical and Subtropical Agriculture CRSR-99-34135-8478.

References

ALI, S.M., FAROOQUI, M.N. & SURYAWANSHI, M.V. (1970). *Myolaimus indicus* n. sp. (Rhabditida: Myolaimidae) and *Metadorylaimus coomansi* n. sp. (Dorylaimida: Tylencholaimidae) from Marathwada, India. *Nematologica* 16, 577-583.

ANDRÁSSY, I. (1959). Weitere Nematoden aus Tropfsteinhohle "Baradla". *Acta Zoological Academiae Scientiarum Hungaricae* 5, 1-6.

ANDRÁSSY, I. (1984). *Klasse Nematoda*. Stuttgart, Germany, Gustav Fischer Verlag, 509 pp.

ANDRÁSSY, I. (2005). *Free-living nematodes from Hungary (Nematoda errantia), I. Pedozoologica Hungarica 3*. Hungarian Natural History Museum and Systematic Zoology Research Group of the Hungarian Academy of Sciences, Budapest, 518 pp.

BALDWIN, J.G., FRISSE, L.M., VIDA, J.T., EDDLEMAN, C.D. & THOMAS, W.K. (1997a). An evolutionary framework for the study of developmental evolution in a set of ne-

matodes related to *Caenorhabditis elegans*. *Molecular Phylogenetics and Evolution* 8, 249-259.

BALDWIN, J.G., GIBLIN-DAVIS, R.M., EDDLEMAN, C.D., WILLIAMS, D.S., VIDA, J.T. & THOMAS, W.K. (1997b). Buccal capsule of *Aduncospiculum halicti* (Nemata: Diplogasterina): an ultrastructural and molecular study with implications for phylogeny. *Canadian Journal of Zoology* 33, 407-423.

BLAXTER, M.L., DE LEY, P., GAREY, J.R., LIU, L.X., SCHELDEMAN, P., VIERSTRAETE, A., VANFLETEREN, J.R., MACKEY, L.Y., DORRIS, M., FRISSE, L.M., VIDA, J.T. & THOMAS, W.K. (1998). A molecular evolutionary framework for the phylum Nematoda. *Nature* 392, 71-75.

BUMBARGER, D.J., CRUM, J., ELLISMAN, M.H. & BALDWIN, J.G. (2006). Three-dimensional reconstruction of the nose epidermal cells in the microbial feeding nematode, *Acrobeles complexus* (Nematoda: Rhabditida). *Journal of Morphology* 267, 1257-1272.

BUMBARGER, D.J., CRUM, J., ELLISMAN, M.H. & BALDWIN, J.G. (2007). Three-dimensional fine structural reconstruction of the nose sensory structures of *Acrobeles complexus* compared to *Caenorhabditis elegans* (Nematoda: Rhabditida). *Journal of Morphology* 268, 649-663.

BYERS, G.W. (1983). The crane fly genus *Chionea* in North America. *The University of Kansas Science Bulletin* 52, 59-195.

COBB, N.A. (1920). One hundred new nemas. *Contributions to a Science of Nematology* 9, 217-343.

DE LEY, P. & BLAXTER, M.L. (2002). Systematic position and phylogeny. In: Lee, D. (Ed.). *The biology of nematodes*. London, UK, Taylor & Francis, pp. 1-30.

DE LEY, P., VAN DE VELDE, M.C., MOUNTPORT, D., BAUJARD, P. & COOMANS, A. (1995). Ultrastructure of the stoma in Cephalobidae, Panagrolaimidae and Rhabditidae, with a proposal for a revised stoma terminology in Rhabditida (Nematoda). *Nematologica* 41, 153-182.

FELIX, M., DE LEY, P., SOMMER, R.J., FRISSE, L., NADLER, S.A., THOMAS, W.K., VANFLETEREN, J. & STERNBERG, P.W. (2000). Evolution of vulva development in the Cephalobina (Nematoda). *Developmental Biology* 221, 68-86.

FÜRST VON LIEVEN, A., BÄRMANN, V. & SUDHAUS, W. (2005). How can nematodes mate without spicules? Function of the male gonoduct glands in the roundworm *Myolaimus*. *Zoology* 108, 211-216.

GIBLIN-DAVIS, R.M. (1997). Phoresy between *Myolaimus heterurus* and a crane fly, *Limonia* (*Rhipdia*) *schwarzi*. *Journal of Nematology* 29, 579. [Abstr.]

GIBLIN-DAVIS, R.M., YE, W., KANZAKI, N., WILLIAMS, D., MORRIS, K. & THOMAS, W.K. (2006). Stomatal ultrastructure, molecular phylogeny and description of *Parasitodiplogaster laevigata* sp. n. (Nematoda: Diplogastridae), a parasite of fig wasps. *Journal of Nematology* 38, 137-149.

GOODEY, T. (1929). On some new and little-known free-living nematodes. *Journal of Helminthology* 1, 27-62.

HIRSCHMANN, H. (1952). Die Nematoden der Wassergrenze mittlefränkischer Gewässer. *Zoologische Jahrbücher (Systematik)* 81, 313-407.

HNATEWYTSCH, B. (1929). Die Fauna der Erzgruben von Schneeberg im Erzgebirge. *Zoologische Jahrbücher (Systematik)* 56, 173-261.

HOLOVACHOV, O. & BOSTRÖM, S. (2006). Description of *Deleyia* gen. n. with a discussion of its phylogenetic relationships to the genera *Daubaylia* Chitwood & Chitwood, 1934 and *Myolaimus* Cobb, 1920 (Nematoda: Rhabditida). *Nematology* 8, 223-233.

JOHANSEN, D.A. (1940). *Plant microtechnique*. New York, USA, McGraw-Hill, 523 pp.

KIMBLE, J. & WARD, S. (1988). Germ-line development and fertilization. In: Wood, W.B. (Ed.). *The nematode* Caenorhabditis elegans. Cold Spring Harbor, NY, USA, Cold Spring Harbor Laboratory Press, pp. 191-213.

KIONTKE, K. & SUDHAUS, W. (2000). Phasmids in male Rhabditida and other secernentean nematodes. *Journal of Nematode Morphology and Systematics* 3, 1-37.

KÖRNER, H. (1954). Die Nematodenfauna des vergehenden Holzes und ihre Beziehungen zu den Insekten. *Zoologische Jahrbücher (Systematik)* 82, 245-353.

MEYL, A.H. (1954). Die Nematodenfauna höherer Pilze in Laub- und Nadelwälden zwischen Braunschweig und dem Harz. *Mycopathologia et Mycologia Applicata* 7, 1-80.

NADLER, S.A., DE LEY, P., MUNDO-OCAMPO, M., SMYTHE, A.B., STOCK, S.P., BUMBARGER, D., ADAMS, B.J., DE LEY, I.T., HOLOVACHOV, O. & BALDWIN, J.G. (2006). Phylogeny of Cephalobina (Nematoda): Molecular evidence for recurrent evolution of probolae and incongruence with traditional classifications. *Molecular Phylogenetics and Evolution* 40, 696-711.

PAESLER, F. (1956). Beitrag zur Erweiterung der Kenntnis der Gattung *Myolaimus*. *Zoologischer Anzeiger* 157, 223-231.

POINAR JR, G.O. (1975). *Entomogenous nematodes: a manual and host list of insect-nematode associations.* Leiden, The Netherlands, E.J. Brill, 317 pp.

PRITCHARD, G. (1983). Biology of Tipulidae. *Annual Review of Entomology* 28, 1-22.

RAGSDALE, E.J., CRUM, J., ELLISMAN, M.H. & BALDWIN, J.G. (2008). Three-dimensional reconstruction of the stomatostylet and anterior epidermis in the nematode *Aphelenchus avenae* (Nematoda: Aphelenchidae) with implications for the evolution of parasitism. *Journal of Morphology* 269, 1181-1196.

RAGSDALE, E.J., NGO, P.T., CRUM, J., ELLISMAN, M.H. & BALDWIN, J.G. (2009). Comparative, three-dimensional anterior sensory reconstruction of *Aphelenchus avenae* (Nematoda: Tylenchomorpha). *Journal of Comparative Neurology* 517, 616-632.

RAHM, G. (1928). Alguns nematodes parasitas e semi-parasitas das plantas culturaes do Brasil. *Archivos do Instituto Biologico* 1, 239-252.

SANWAL, K.C. (1960). *Macrolaimus canadensis* n. sp. (Nematoda: Panagrolaimidae), from the frass of the bark beetle *Phloeosinus canadenis* Swaine, 1917, with remarks on other species of the genus *Macrolaimus* Maupas, 1900. *Canadian Journal of Zoology* 38, 1127-1131.

SCHIERENBERG, E. (1984). Altered cell-division rates after laser-induced cell fusion in nematode embryos. *Developmental Biology* 101, 240-245.

SOMMER, R.J. (2005). Evolution of development in nematodes related to *C. elegans* (December 14, 2005), WormBook, ed. The *C. elegans* Research Community, WormBook, doi/10.1895/wormbook.1.46.1. Available online at http://www.wormbook.org

SOUTHEY, J.F. (1970). *Laboratory methods for work with plant and soil nematodes*. London, UK, Her Majesty's Stationery Office, 148 pp.

SUDHAUS, W. (1977). *Rhabditis dimorpha*: ein Beispiel für unvollständige Häutung und Sexualdimorphismus bei Nematoden. *Zoologischer Anzeiger* 199, 325-352.

VAN DE VELDE, M.C., DE LEY, P., MOUNPORT, D., BAUJARD, P. & COOMANS, A. (1994). Ultrastructure of the buccal cavity and the cuticle of three Cephalobidae (Nematoda: Rhabditida). *Nematologica* 40, 541-563.

WARD, S., THOMSON, N., WHITE, J.G. & BRENNER, S. (1975). Electron microscopical reconstruction of the anterior sensory anatomy of the nematode *Caenorhabditis elegans*. *Journal of Comparative Neurology* 160, 313-337.

WEINGÄRTNER, I. (1952). Die Nematoden des Kompostes. *Sitzungsberichte der physikalisch-medizinischen Societät in Erlangen* 76, 86-107.

WHITE, J. (1988). The anatomy. In: Wood, W.B. (Ed.). *The nematode Caenorhabditis elegans*. Cold Spring Harbor, NY, Cold Spring Harbor Laboratory Press, pp. 81-122.

WHITE, J.G., SOUTHGATE, E., THOMSON, J.N. & BRENNER, S. (1986). The structure of the nervous system of *Caenorhabditis elegans*. *Philosophical Transactions of the Royal Society of London B* 341, 1-340.

WILLAMS, B.D., SCHRANK, B., HUYNH, C., SHOWNKEEN, R. & WATERSON, R.H. (1992). A genetic mapping system in *Caenorhabditis elegans* based on polymorphic sequence-tagged sites. *Genetics* 131, 609-624.

YE, W., GIBLIN-DAVIS, R.M., BRAASCH, H., MORRIS, K. & THOMAS, W.K. (2007). Phylogenetic relationships among *Bursaphelenchus* species (Nematoda: Parasitaphelenchidae) inferred from nuclear ribosomal and mitochondrial DNA sequence data. *Molecular Phylogenetics and Evolution* 43, 1185-1197.

YUSHIN, V.V. & MALAKHOV, V.V. (2004). Spermatogenesis and nematode phylogeny. In: Cook, R. & Hunt, D.J. (Eds). *Proceedings of the 4th International Congress of Nematology, Tenerife, Spain, 8-13 June 2002, Nematology Monographs and Perspectives, Volume 2*. Leiden, The Netherlands, Brill, pp. 655-665.